"WEAK AND SMART" MAGNETIC DEFECTS IN IRON PNICTIDES

K. Kikoin*

Tel Aviv University

*with
S. Drechsler (Dresden)
J. van der Brink (Dresden)
K. Koepernik (Dresden)
J. Malek (Prague)
V. Grinenko (Dresden)
M. Kiselev (Trieste)
D. Efremov (Stuttgart/ Dresden)

- Phys. Rev. B **83**, 134516 (2011)
- J. Magn. Magn. Mater. **324**, 3471 (2012)
- Nature Sci. Rep. **5**, 11280 (2015)
- arXiv:1601.03552

Specifically: **$La0_{0.9}F_{0.1}FeAs_{1-x}$**

Other examples: **As** deficient **Ba-221; Ru** and Zn doped **La-1111 …**

Problem: Non-stoichiometric La(O,F)FeAs samples with 5-10% As vacancies demonstrate quite unusual magnetic properties, as if V_{As} was magnetic impurity.

- What is the microscopic reason of such counter intuitive behavior of As vacancies?
- How do V_{As} defects influence magnetic response?
- How do V_{As} defects influence Cooper pairing?

Basic experimental findings:

Nuclear Spin Lattice Relaxation Rate $1/T\,T_1\,(T)$:
Expected behavior: ~ Const + aT^2 at $T > T_c$
~ exp $(-\Delta/T)$ at $T < T_c$

Instead, something like ~ T^5 below T_c and linear above T_c it demonstrates response of a metal with extrinsic local moments.

Deviation from gap-wise behavior at $T < T_c$ could be ascribed to nodes in the SC gap, but this is apparently not the case in (1111) systems.

More reasonable mechanism is filling of the gap due to defect-related states. **But why** the gap becomes "cleaner" in non-stoichiometric samples ???

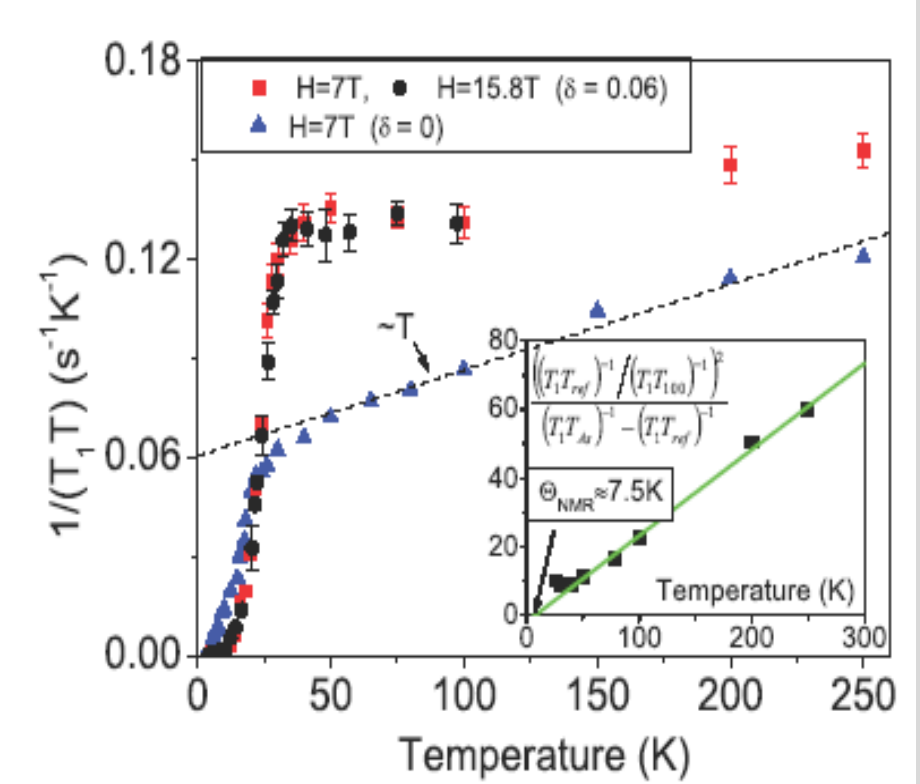

* F. Hammerath, S. Drechsler, H.-J. Grafe, G. Lang, G. Fuchs, G. Behr, I. Eremin, M. Korshunov, B. Bűchner

Phys. Rev. B **81**, 140504(R) (2010)

More detailed studies of magnetic response in normal state: (*Grinenko et al, '11*)

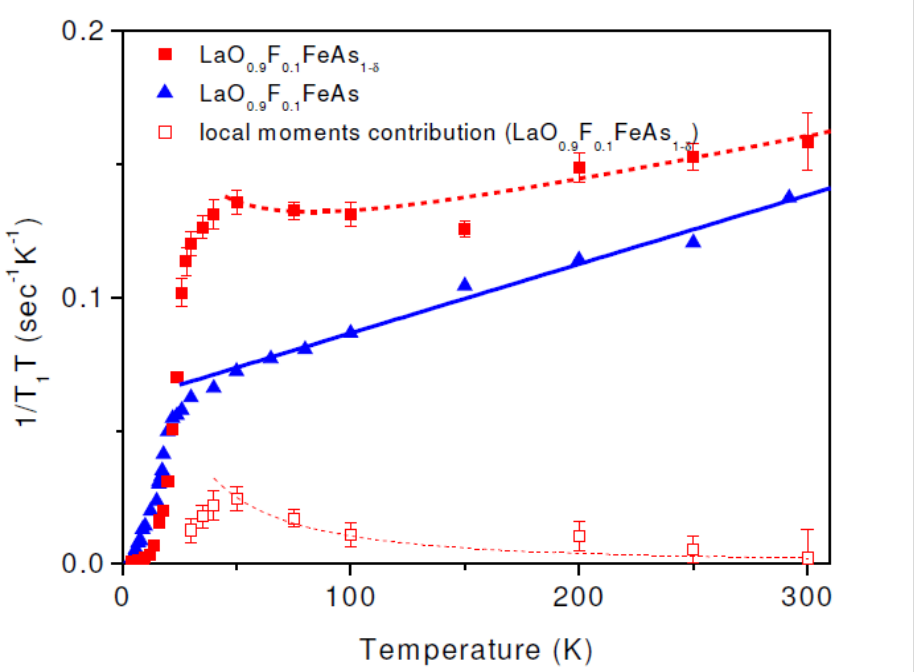

- A hump in temperature dependence of $\int \chi_q(\omega)\, d\mathbf{q}$, $\omega \to 0$, measured by NSLR

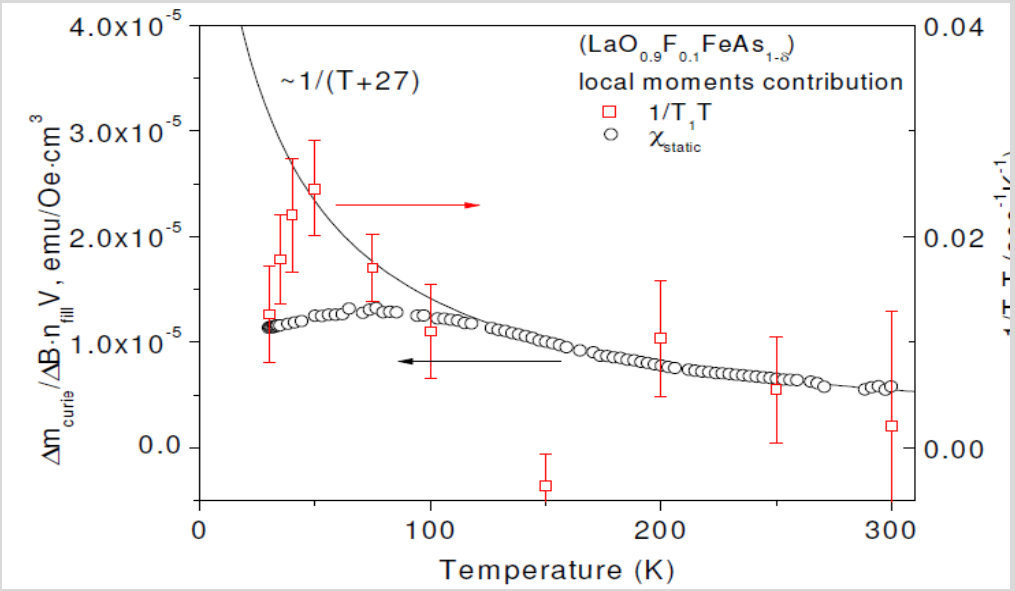

- Nearly similar hump in static susceptibility measured by SQUID

- Enhanced paramagnetic susceptibility responsible for appearance of the Pauli limiting field B_{c2} which is absent in stoichiometric samples

Measured magnetization

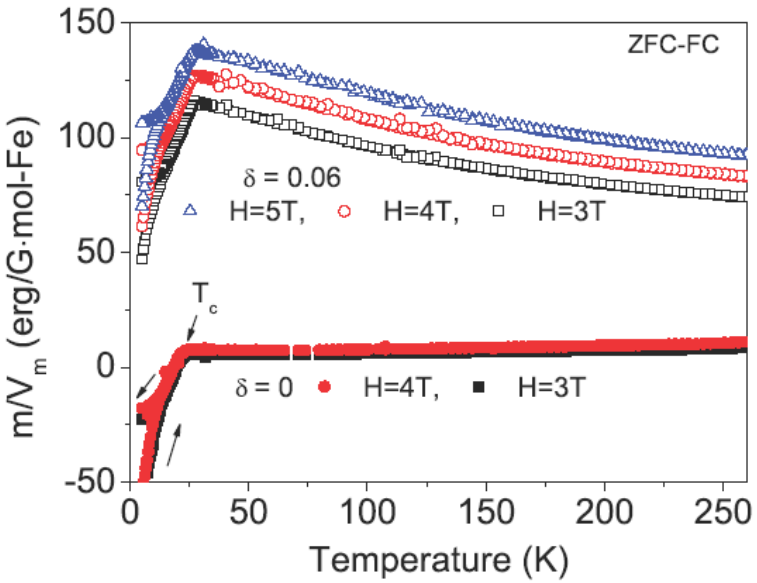

FIG. 3: (color online) Temperature dependence of the magnetization after zero-field cooling at different magnetic fields for $LaO_{0.9}F_{0.1}FeAs_{1-\delta}$.

Predecessors:

contribution of ”static paramagnetic spin clusters” in μSR spectra of As deficient 1111 superconductor (*G. Fuchs, S. Drechsler, H-H Klauss et al.* (2009)

Measured susceptibility

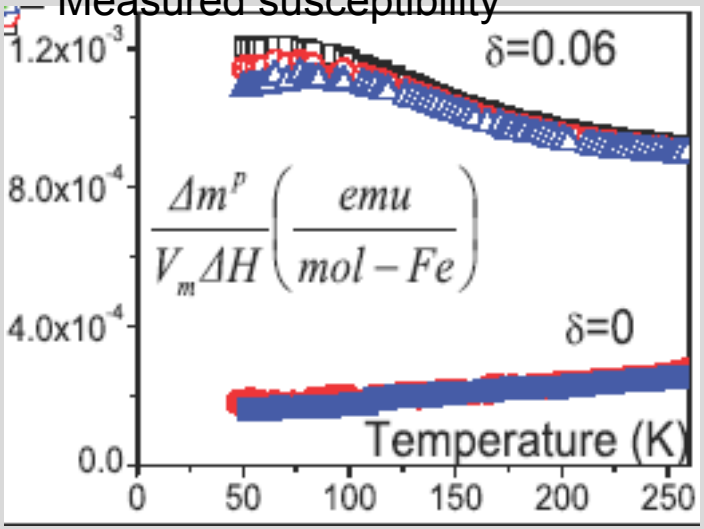

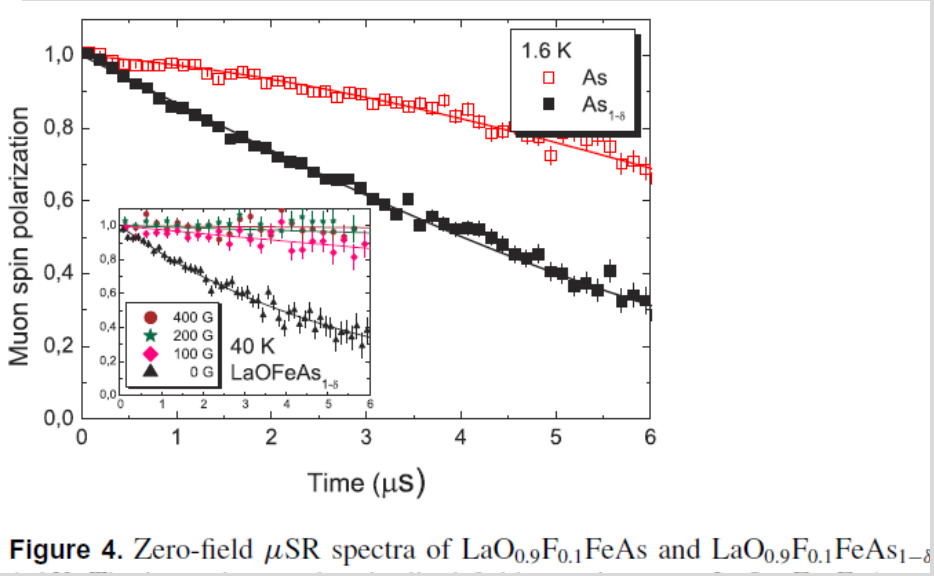

Figure 4. Zero-field μSR spectra of $LaO_{0.9}F_{0.1}FeAs$ and $LaO_{0.9}F_{0.1}FeAs_{1-\delta}$

Similar effects are observed in Zn doped 1111 compounds. Later we will see that this similarity is not accidental.

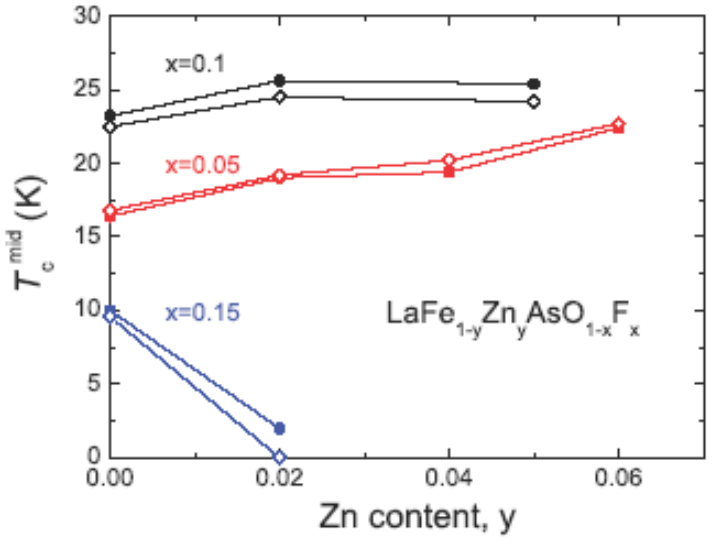

Figure 4. (color online) Superconducting transition temperatures versus Zn content in $LaFe_{1-y}Zn_yAsO_{1-x}F_x$. Solid and open symbols refer to T_c determined from the measurements of resistivity (midpoint) and susceptibility (onset point), respectively. The data of $x = 0.1$ were taken from the previous report.[19]

Similar defects in 122 family

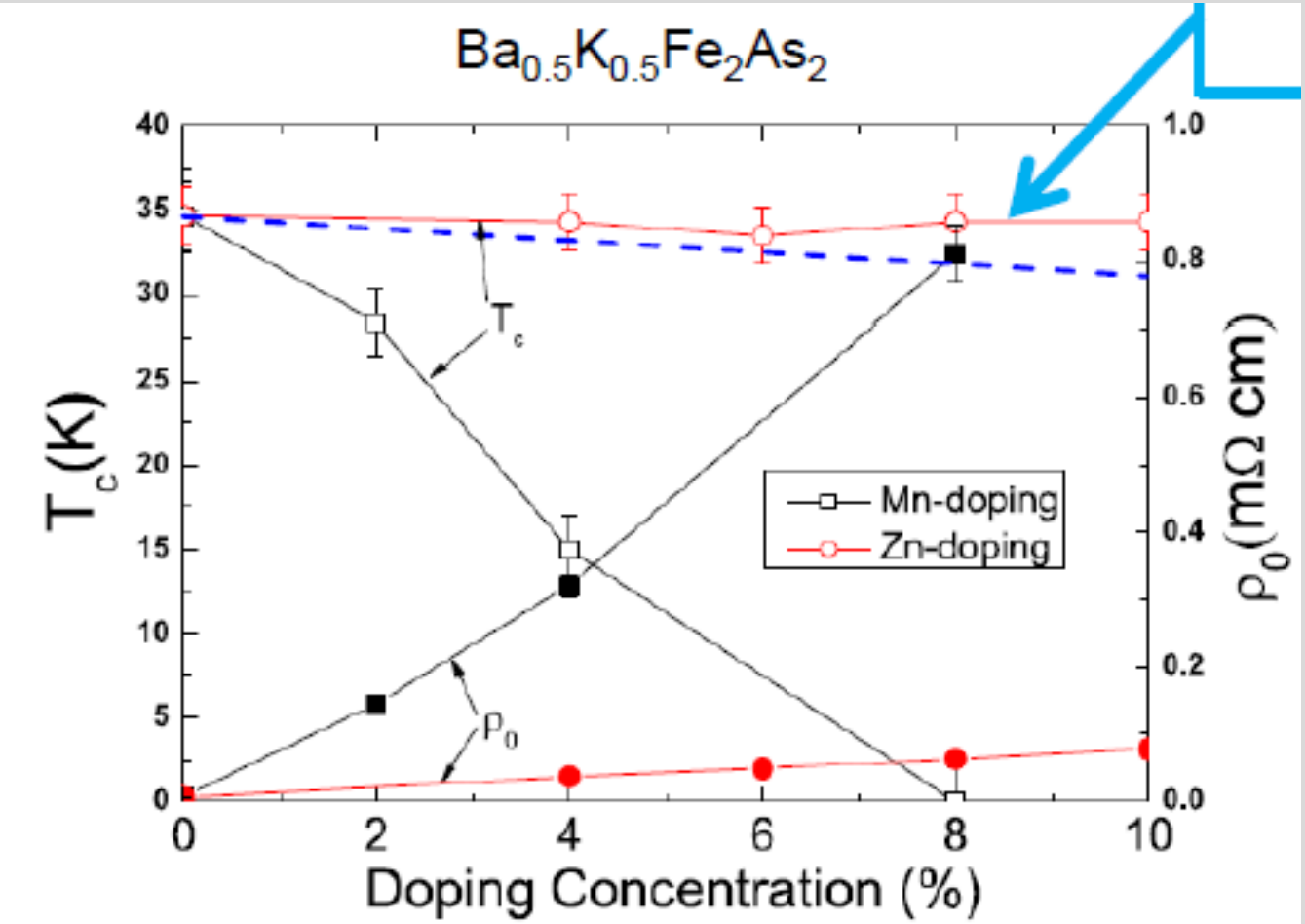

Basic structural information about iron pnictides and chalcogenides

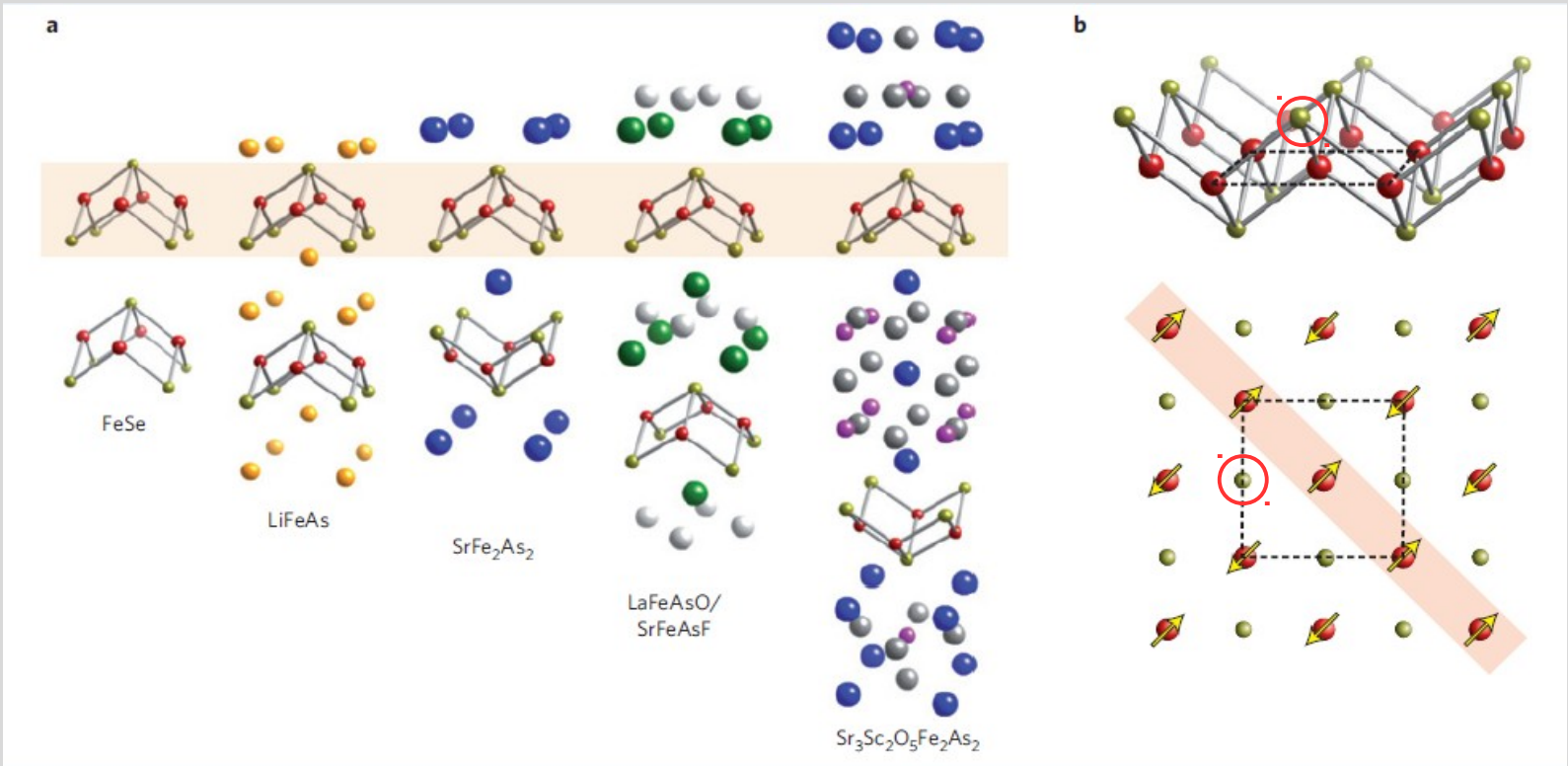

Figure B1 | Crystallographic and magnetic structures of the iron-based superconductors. a, The five tetragonal structures known to support superconductivity. **b**, The active planar iron layer common to all superconducting compounds, with iron ions shown in red and pnictogen/chalcogen

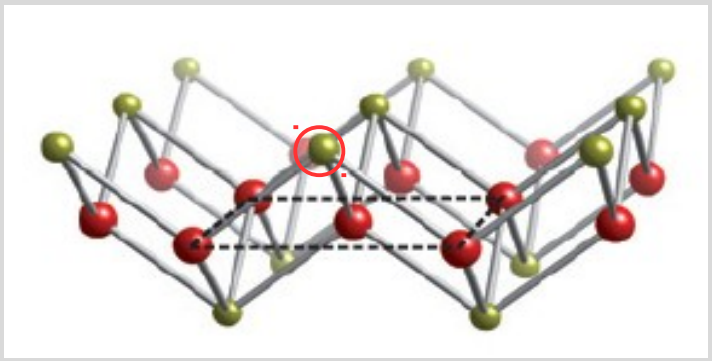

<u>As vacancy:</u>

- Creates a defect in As related chemical bonds
- Creates **dangling bond defects** in d-b hybridized orbitals

Phase diagram (1111 system)

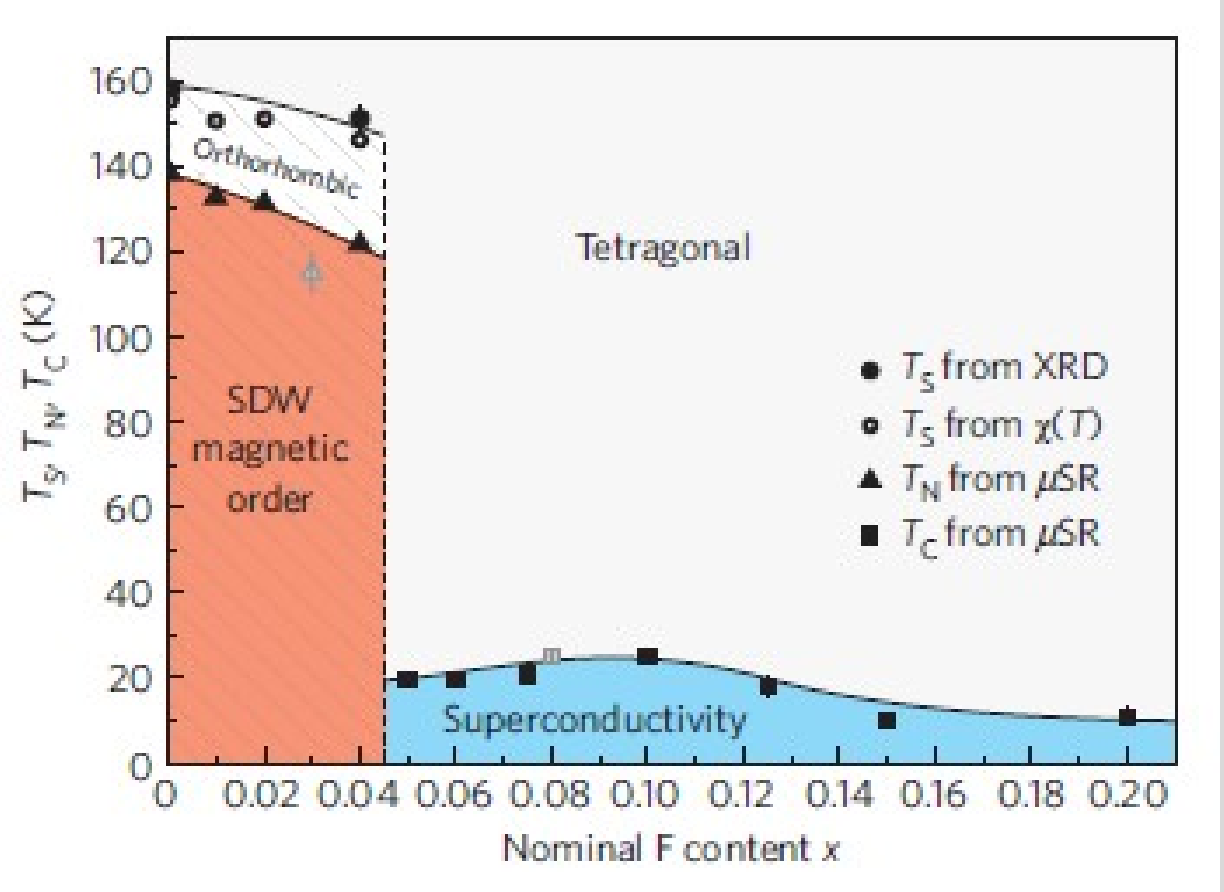

(*Leutkens et al '09*)

Phase diagram (122 systems)

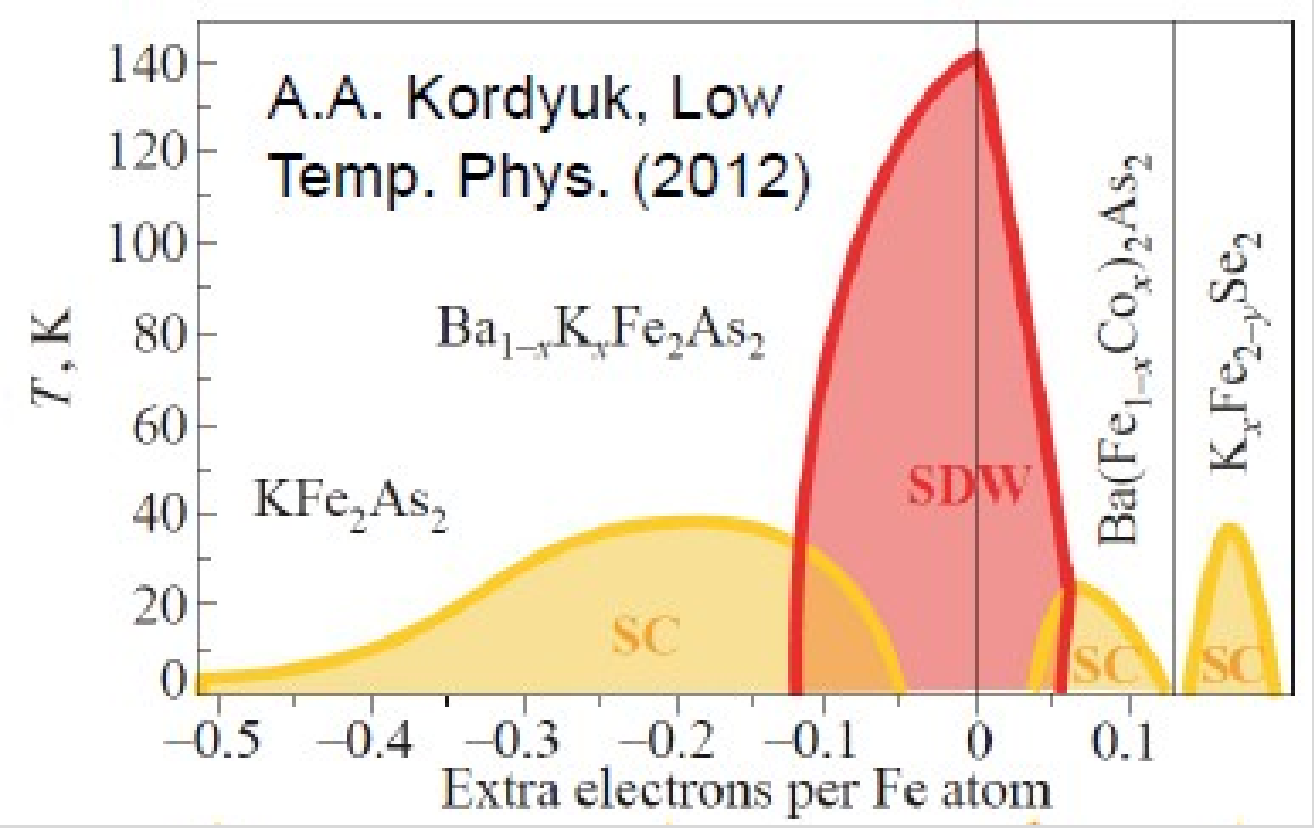

Generic phase diagram for electron- and hole-doped iron pnictides

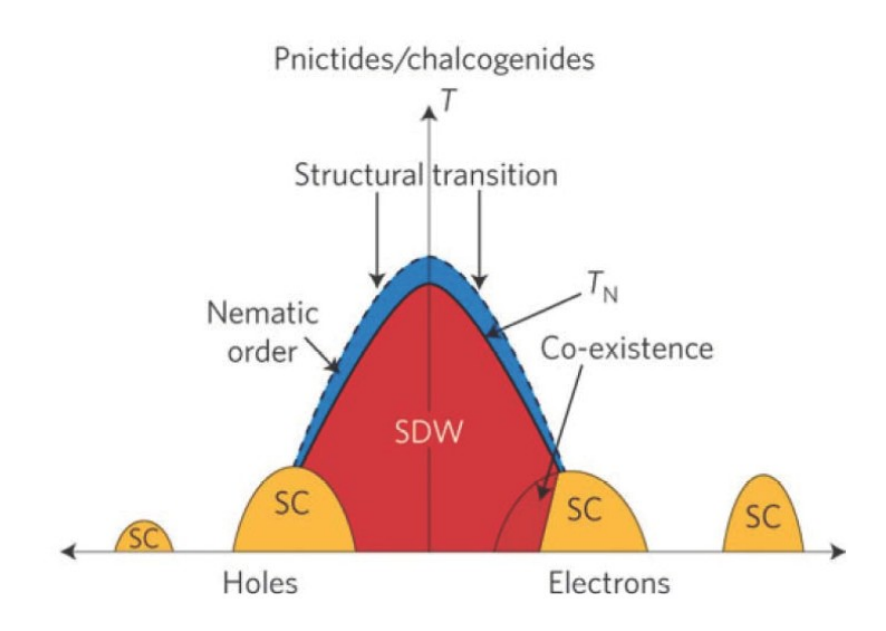

paradigmatic (*Chubukov '11*)

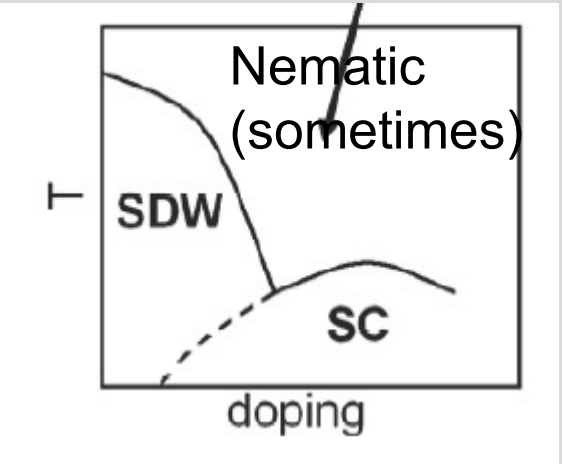

SDW emerges due to nesting between hole and electron pockets at FS. Doping makes nesting imperfect, so that only SDW fluctuations survive. These fluctuations mediate Cooper pairing.

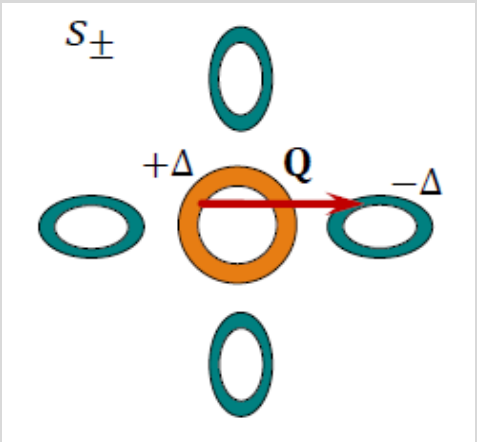

Basic information about electronic structure (*H.Eschrig and K.Koepernik, '09*)

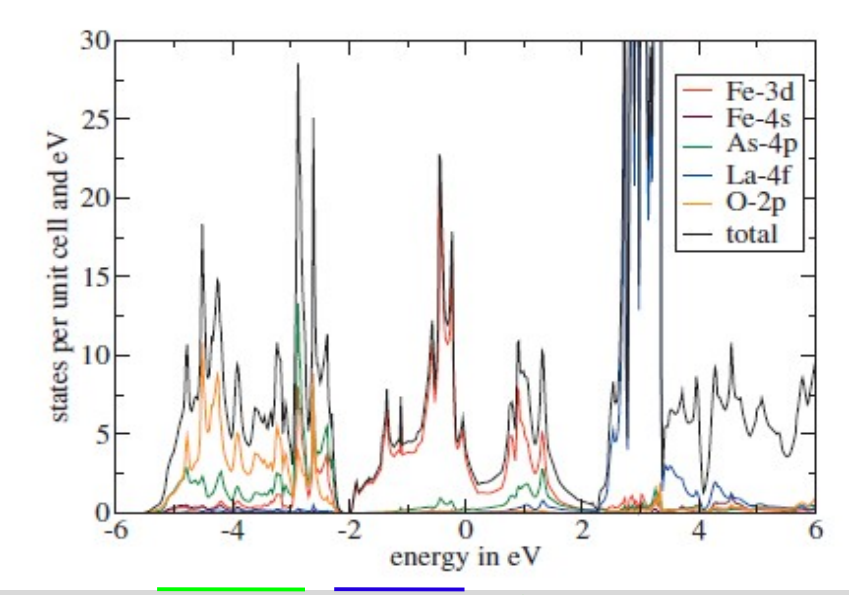

p d + p

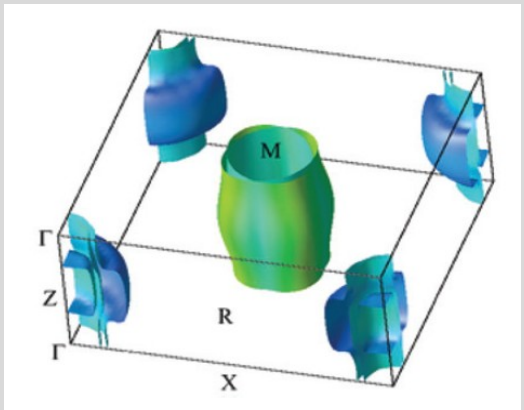

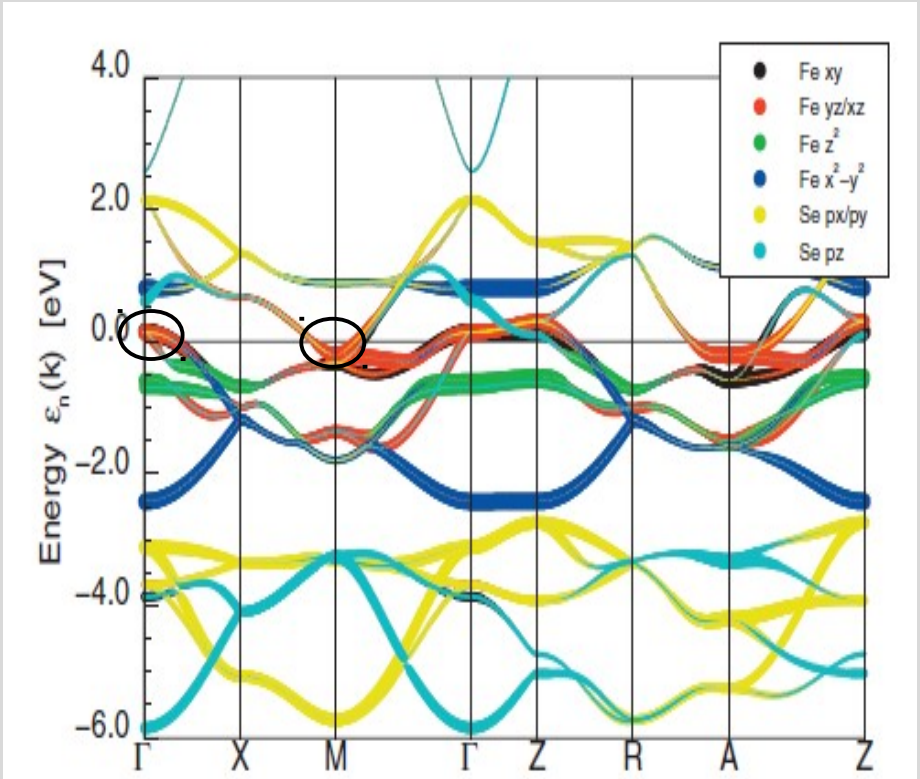

FIG. 6. (Color) Orbital projection of the LDA band structure of FeSe. (See Fig. 9 for the points Γ, *X*, *M*; *Z*, *R*, and *A* are above the

Quasi 2D semimetal !

Blow-up of DOS

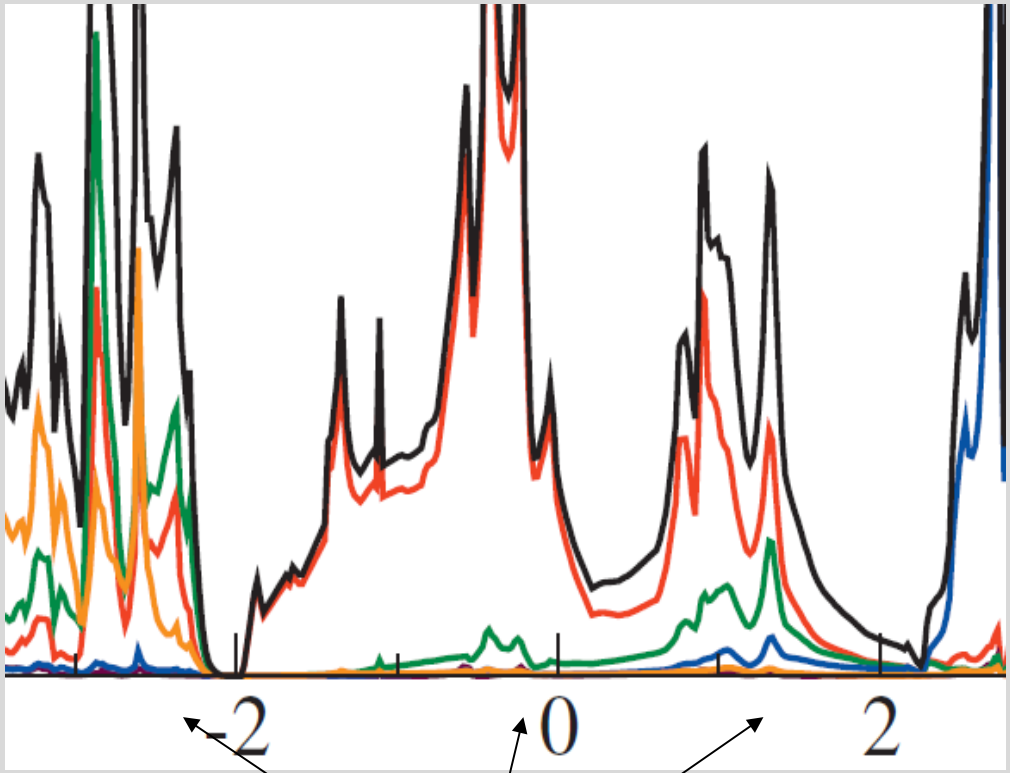

As – 4p partial DOS

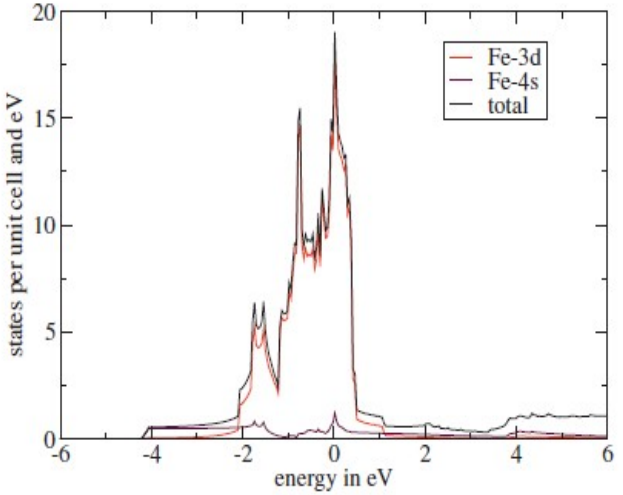

FIG. 7. (Color) Partial and total DOS for a hypothetical structure obtained by removing the Se atoms from FeSe.

Pseudogap around FS arises due to strong covalent dp-bonding!
This fact is a starting point for solving the puzzling activity of As vacancies.

Nocheinmal und langsam: (*Yanagi et al '10*)

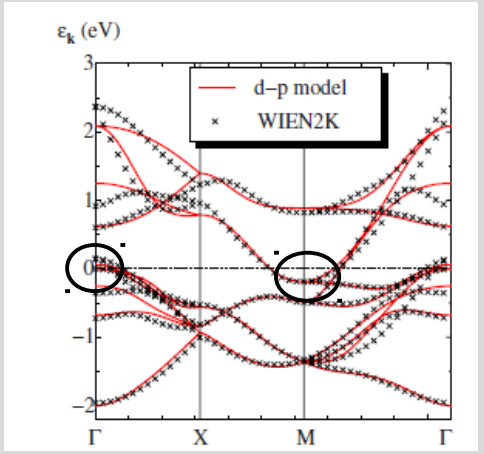

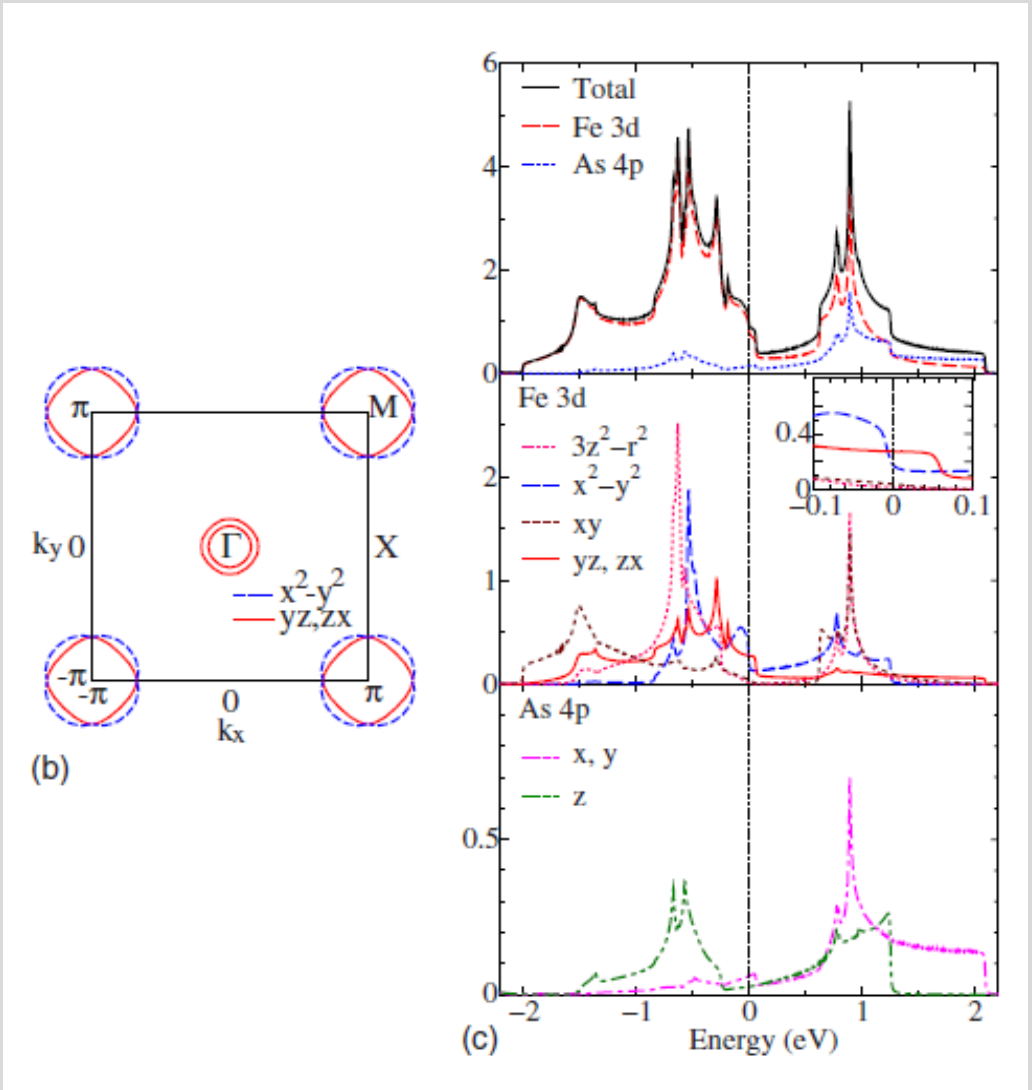

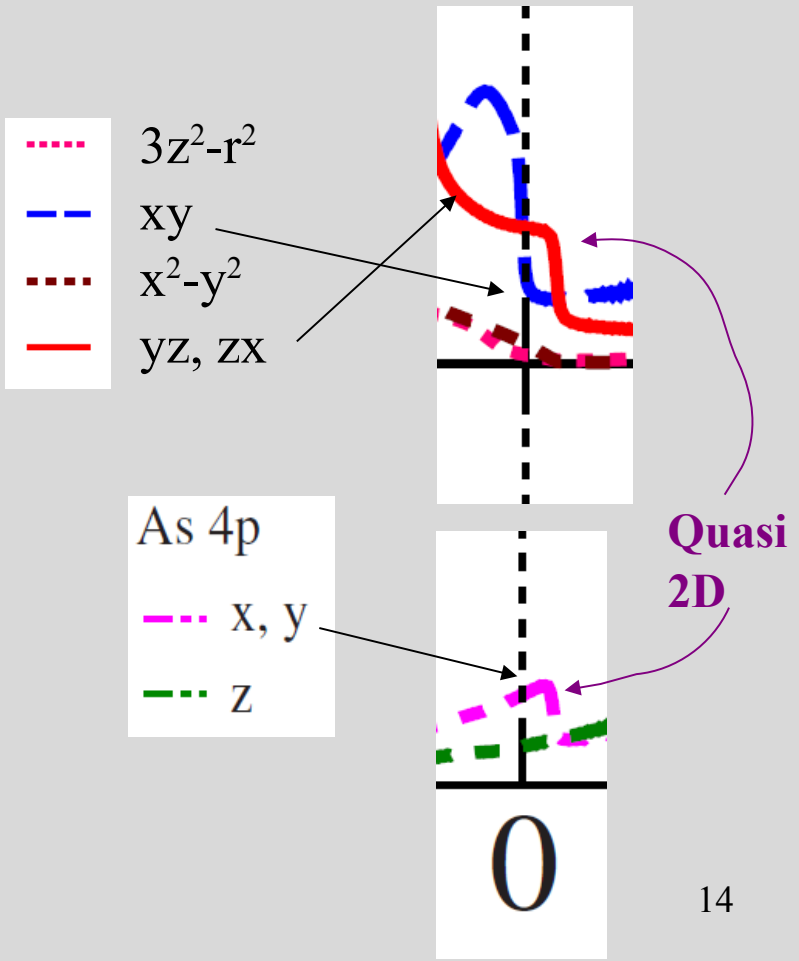

SC pairing mechanism (conjectural)

Nesting vector responsible for SDW correlations between two pockets of FS

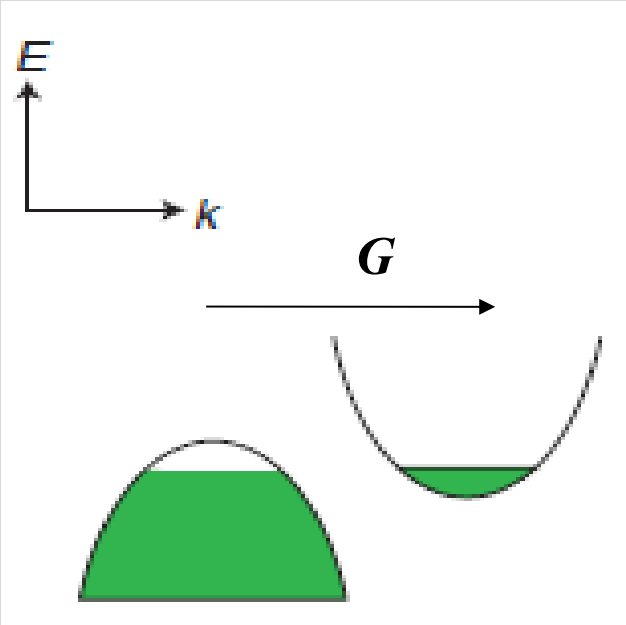

S^{+-} pairing: two nodeless gaps with opposite sign due to phase difference. These gaps see each other via repulsive SDW-mediated interaction [$\chi_q(\omega)$ with $\boldsymbol{q} \sim \boldsymbol{G}$]

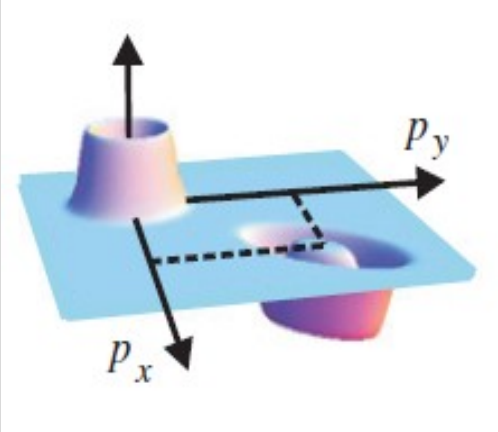

(*Aronov, Sonin '72; Mazin et al '08; Kuroku et al '08*)

IMPURITY SCATTERING vs COOPER PAIRING: COMMON WISDOM

Single band BCS pairing mechanism:

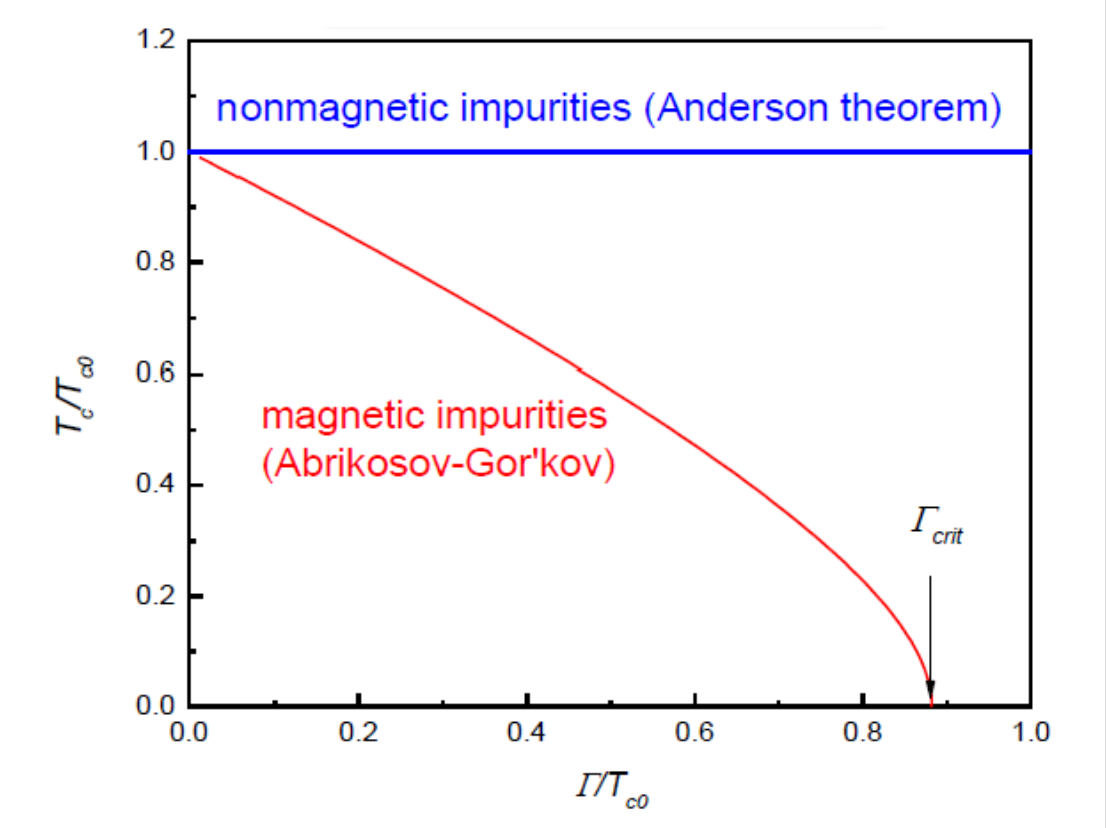

Only quantum number changes. Energy instead of momentum.
k - -**k** ⟶ **n** - -**n**
(time-reversal conjugated);
Dirty limit (*Anderson 1959*)

Spin reversal scattering breaks Cooper pairs. Infrared cutoff of logarithmic divergency in the BCS equation

2-band $s_{\pm}$ system

Potential scattering:

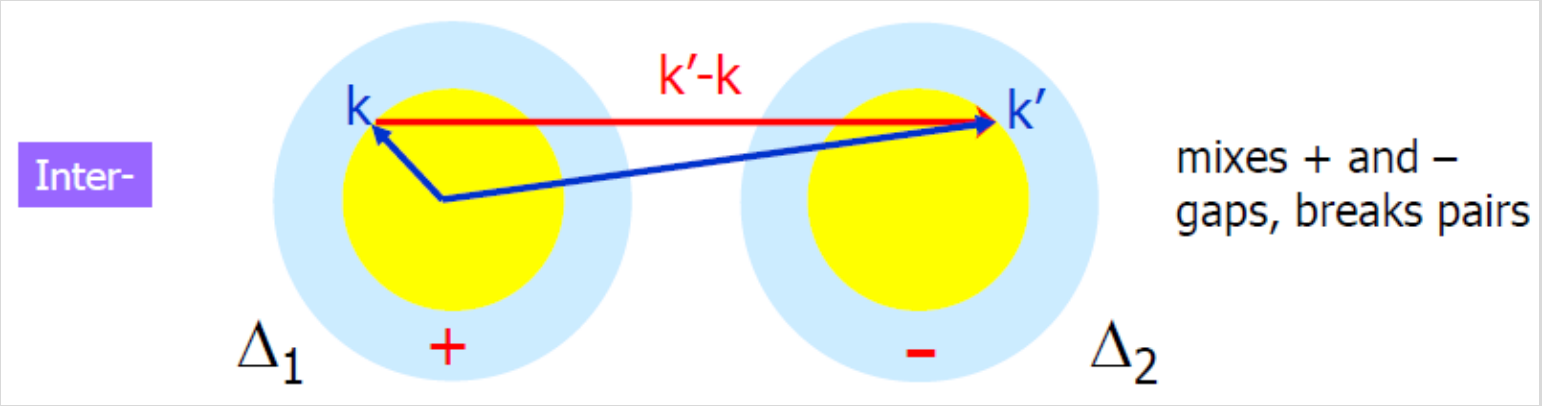

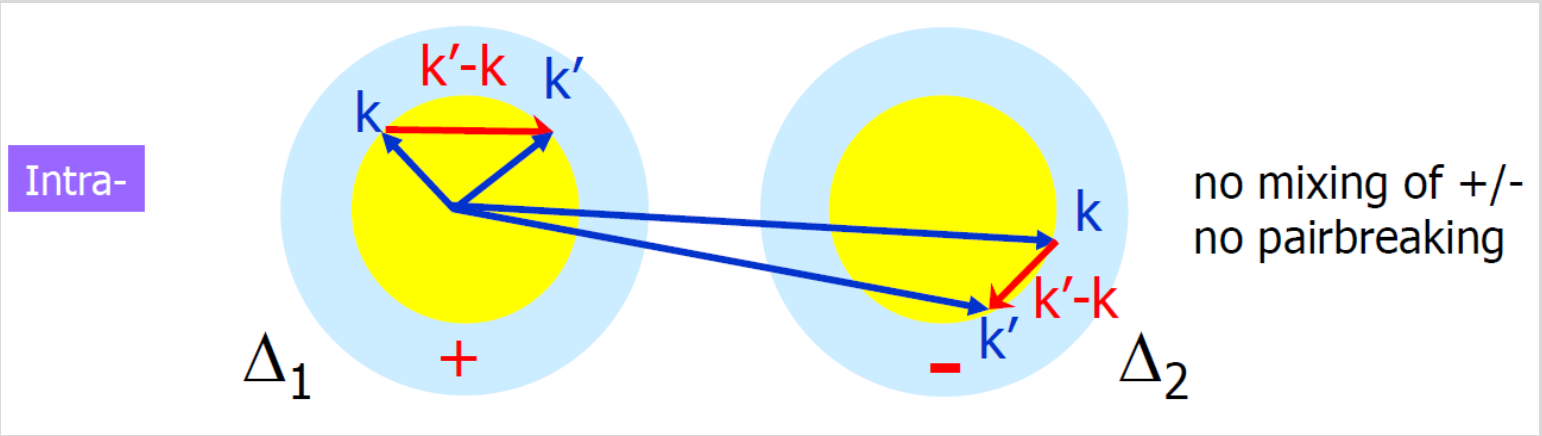

(*borrowed from I.Eremin)*

Minimal model of V_{As} related defect in $LaFeAs_{1-\delta}OF$ iron pnictide

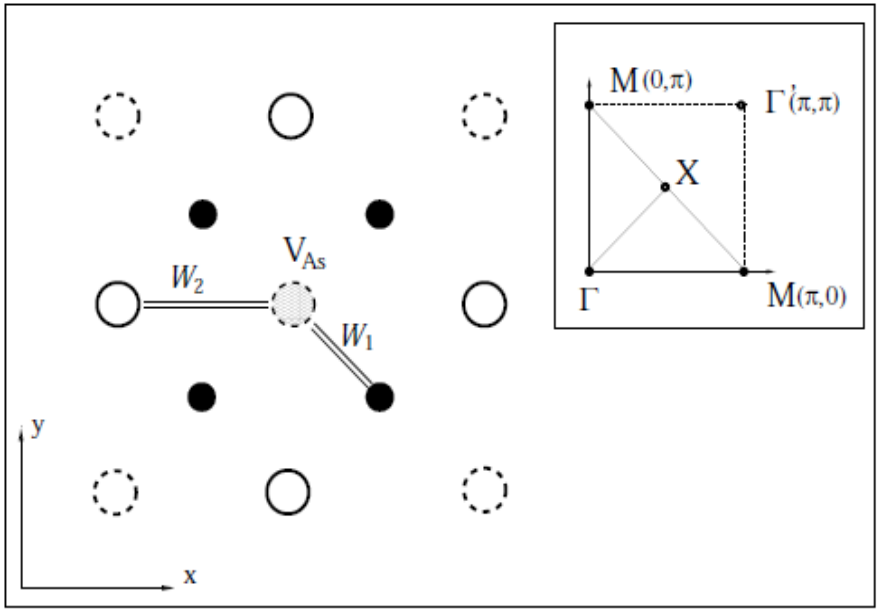

FIG. 1: Bond coordination around As vacancy in Fe-As layer.

$$H = H_d + H_p + H_{dp} + H_{vd} + H_{vp} = \quad (1)$$
$$\sum_{k\sigma} \varepsilon_{k,d} d^\dagger_{k\sigma} d_{k\sigma} + \sum_{k\sigma} \varepsilon_{k,p} p^\dagger_{k\sigma} p_{k\sigma}$$
$$+ \sum_{k\sigma} \left(V_{dp}(k) d^\dagger_{k\sigma} p_{k\sigma} + \text{H.c.} \right)$$
$$+ W_1 \sum_{j\sigma} \left(d^\dagger_{j\sigma} p_{0\sigma} + \text{H.c.} \right) + W_2 \sum_{l\sigma} \left(p^\dagger_{l\sigma} p_{0\sigma} + \text{H.c.} \right)$$

V_{As} is treated as a missing ion As^{3-} which generates dangling bonds with 4 neighboring Fe ions in the central square plane and 4 neigboring As ions packed in tetrahedral coordination. In our minimal tight binding model these bonds are formed by the p-orbitals $p_{x,y} = (p_x \pm p_y)/\sqrt{2}$ and d-orbitals $d_{xz,yz} = (d_{xz} \pm d_{yz})/\sqrt{2}$.

The main term responsible for formation of the defect is

$$H_{vd} = W_1 \sum_k \left[F(k) d^\dagger_{k\sigma} p_{0\sigma} + \text{H.c.} \right]$$

where $F(k) = 4 \cos k_x \cos k_y \exp(ik_z/2)$.

Minimal model (*cont.*)

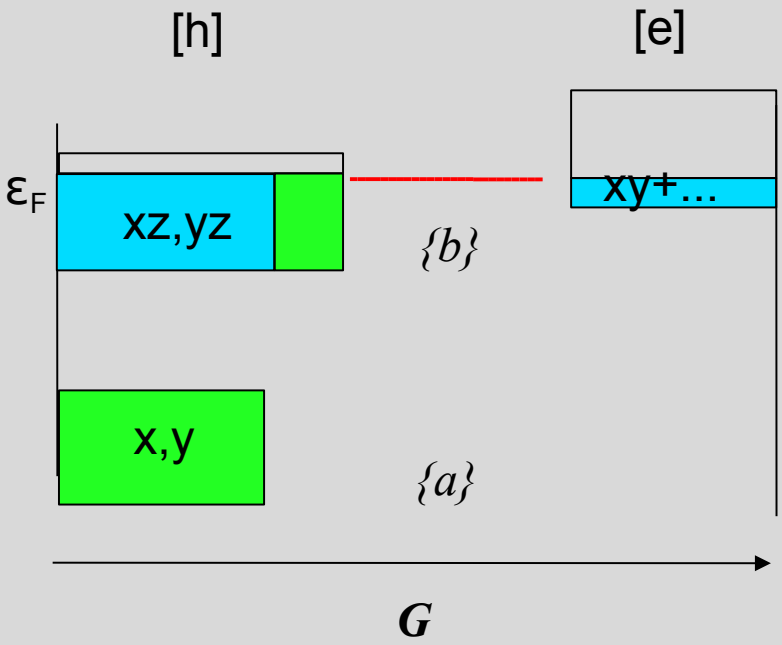

As vacancy: Short-range scattering potential localized within a defect shell.

Dyson equations:

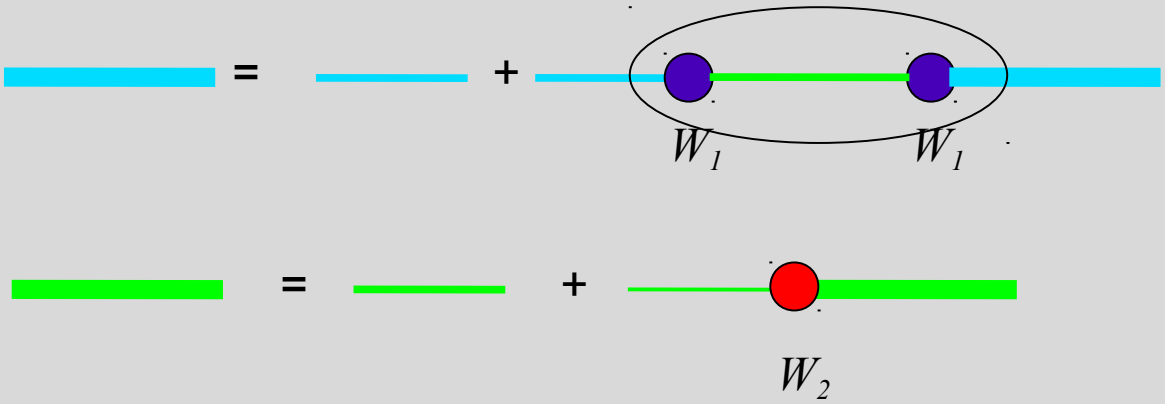

$$\hat{G}_b = \hat{g}_b + \hat{g}_b W_1 \hat{g}_a W_1 \hat{G}_b$$
$$\hat{G}_a = \hat{g}_a + \hat{g}_a W_2 \hat{G}_a$$

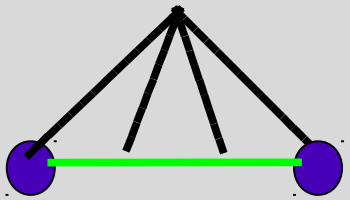

Multiple rescattering (T-matrix)

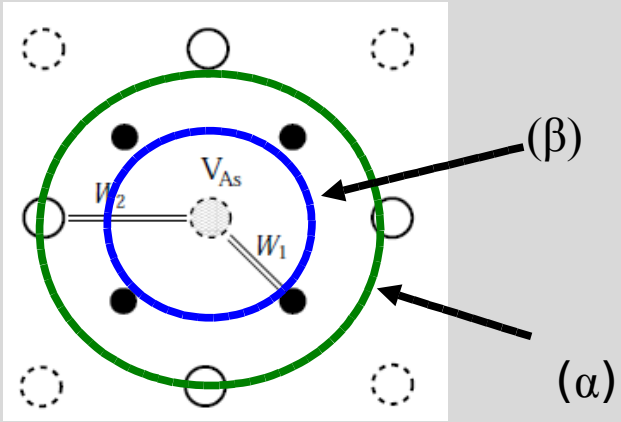

Let us introduce local "molecular orbitals" built from d-Fe and p-As atomic orbitals of defect cell which retain the point symmetry of the Γ point in BZ and project Dyson equations on the local basis {α,β}

The local Green functions G^0 are defined as

$$G^0_{\alpha\alpha}(\omega) = \sum_{\mathbf{k}} \frac{\langle\alpha|\mathbf{k}a\rangle\langle\mathbf{k}a|\alpha\rangle}{\omega - \varepsilon_{\mathbf{k}a}}$$

$$G^0_{\beta\beta}(\omega) = \sum_{\mathbf{k}} \frac{\langle\beta|\mathbf{k}b\rangle\langle\mathbf{k}b|\beta\rangle}{\omega - \varepsilon_{\mathbf{k}b}}$$

$$|\beta\rangle_x = \sum_{j=1}^{4} |d_j\rangle_{yz},$$

$$|\beta\rangle_y = \sum_{j=1}^{4} |d_j\rangle_{xz}$$

"Dangling bond" hybridization parameter

$$W_{\beta\alpha} = \langle\beta|W_1|\alpha\rangle$$

Secular matrix in the local basis {α,β}:
Defect potential affects ***p*-states** and ***dp* bonds**.

$$Q(\epsilon) = \begin{pmatrix} 1 & -W_{1,\alpha\beta} G^0_{\beta\beta}(\epsilon) \\ -W_{1,\beta\alpha} G^0_{\alpha\alpha}(\epsilon) & 1 - W_{2,\alpha\alpha} G^0_{\alpha\alpha}(\epsilon) \end{pmatrix}$$

$$Q_1(\epsilon) = 1 - \sum_\alpha W_{1,\beta\alpha} G^0_{\alpha\alpha}(\epsilon) W_{1,\alpha\beta} G^0_{\beta\beta}(\epsilon) = 0.$$

$$W_{1,\beta} = \sum_\alpha W_{1,\beta\alpha} G^0_{\alpha\alpha}(\epsilon) W_{1,\alpha\beta}.$$

At $\omega \sim \varepsilon_F$ the frequency dependence $U(\omega)$ is very week, and the position of the poles is predetermined by the analytical properties of $G_{\beta\beta}(\omega)$ which is in fact the Hilbert transform of 2D density of states, so that at the band edge

$$\mathrm{Re}\; G^0_{\beta\beta}(\omega \to \varepsilon_t) \propto \nu_0 \ln\left[D/|\omega - \varepsilon_t|\right].$$

We solve graphically equation $W^{-1} = G^0$

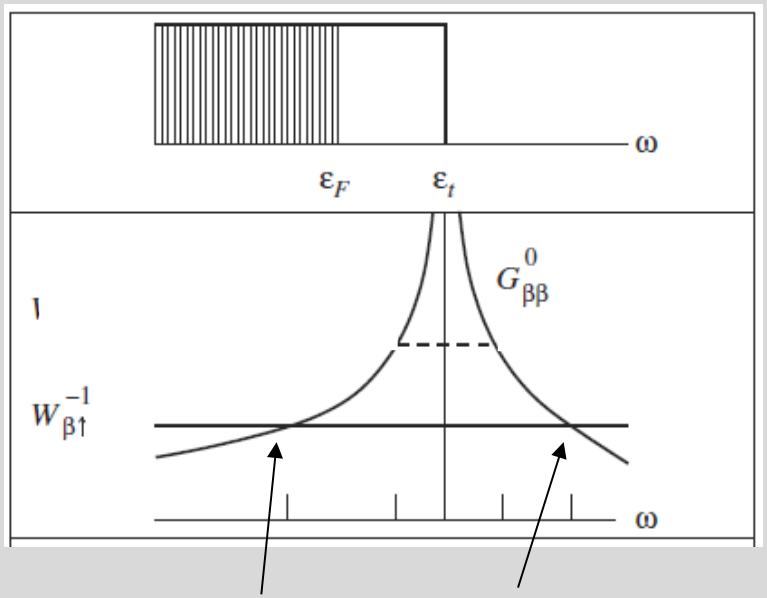

Bare DOS

resonance

antiresonance (empty state)

If the scattering is strong, then one should take into account multiple on-site scattering, i.e. turn to T-matrix

T – matrix is given by the equation

$$\mathcal{T}_{\mathbf{k}\mathbf{k}'} = \frac{F_\beta(\mathbf{k}) W_\beta(\omega) F_\beta(\mathbf{k}')}{1 - W_\beta(\omega) G^0_{\beta\beta}(\omega)},$$

$$W_\beta = \sum_\alpha W_{\beta\alpha} G^0_{\alpha\alpha}(\omega) W_{\alpha\beta}$$

One can judge about the resonances created by the defect in the hole band spectrum from the partial scattering phase

$$\tan \delta_\alpha(\omega) = -\frac{\mathrm{Im} \det \widetilde{Q}(\omega)}{\mathrm{Re} \det \widetilde{Q}(\omega)}$$

$$\widetilde{Q} = 1 - U_\alpha(\omega) G_{\alpha\alpha}(\omega)$$

Zero in denominator means $\delta_\alpha = \pi/2$, i.e. resonance scattering.

Edge singularity guarantees existence of such resonance near the top of the hole band whatever weak is the scattering potential!

This simplified model allows analytical solution.

To make it trustful, we have found V_{As} related spectrum
in a **repeated supercell** (quasiband) first principle DFT calculations.

$$\mathrm{LaOFeAs}_{1-x},\ x = \frac{1}{16}$$

8 formula units in a square arrangement contained 16 Fe atoms
The As atom in the center of the square cell was removed.

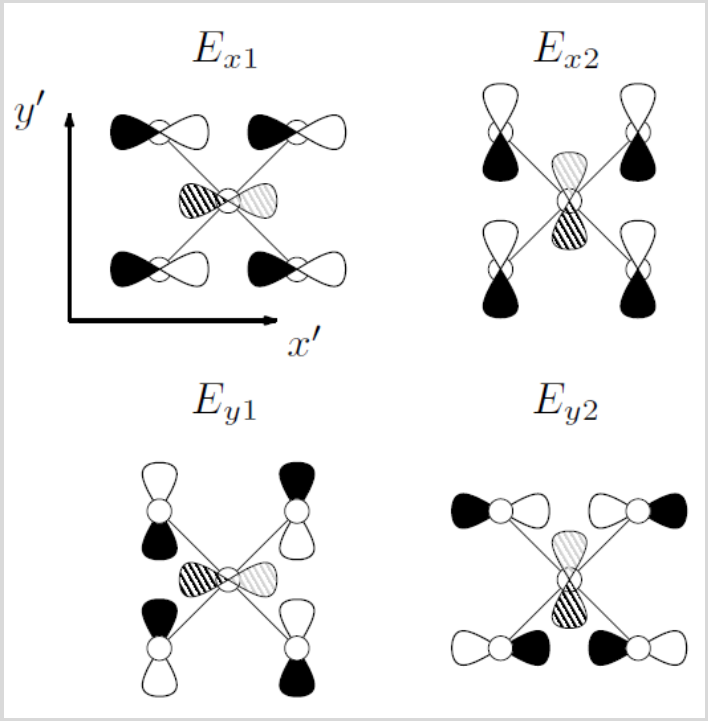

Calculated MO and their partial contribution in the supercell DOS

$$8 \cdot 3\mathrm{d}_{(xy)z} = A_1 + A_2 + B_1 + B_2 + 2E.$$

Only E_x orbitals are hybridized with V_{As} related $p_{x,y}$ orbitals

$$E_{x1} = \frac{1}{2}\left(\Phi_{xz,1-1} + \Phi_{xz,11} + \Phi_{xz,-11} + \Phi_{xz,-1-1}\right)$$
$$E_{x2} = \frac{1}{2}\left(\Phi_{yz,1-1} + \Phi_{yz,11} + \Phi_{yz,-11} + \Phi_{yz,-1-1}\right)$$

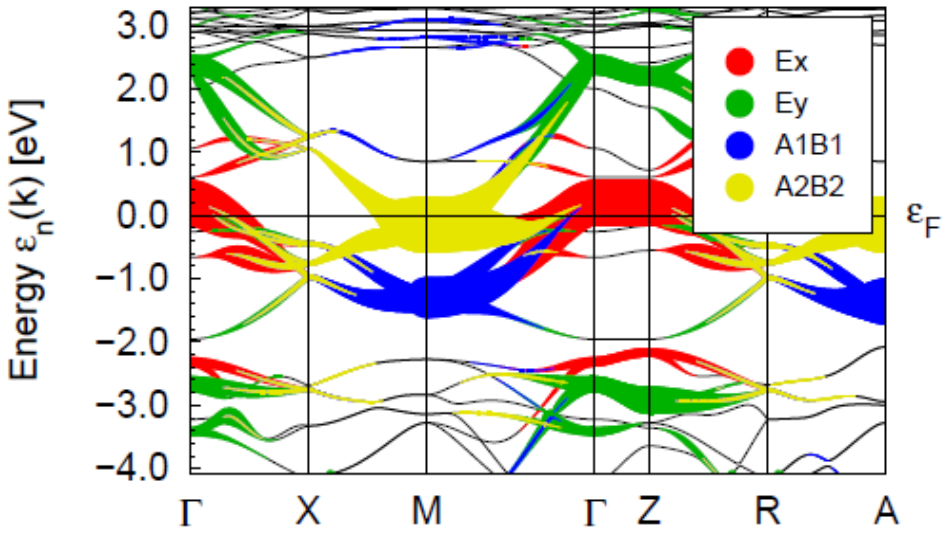

Figure 4: (color online) Molecular orbital projected bands for ordered LaOFeAs.

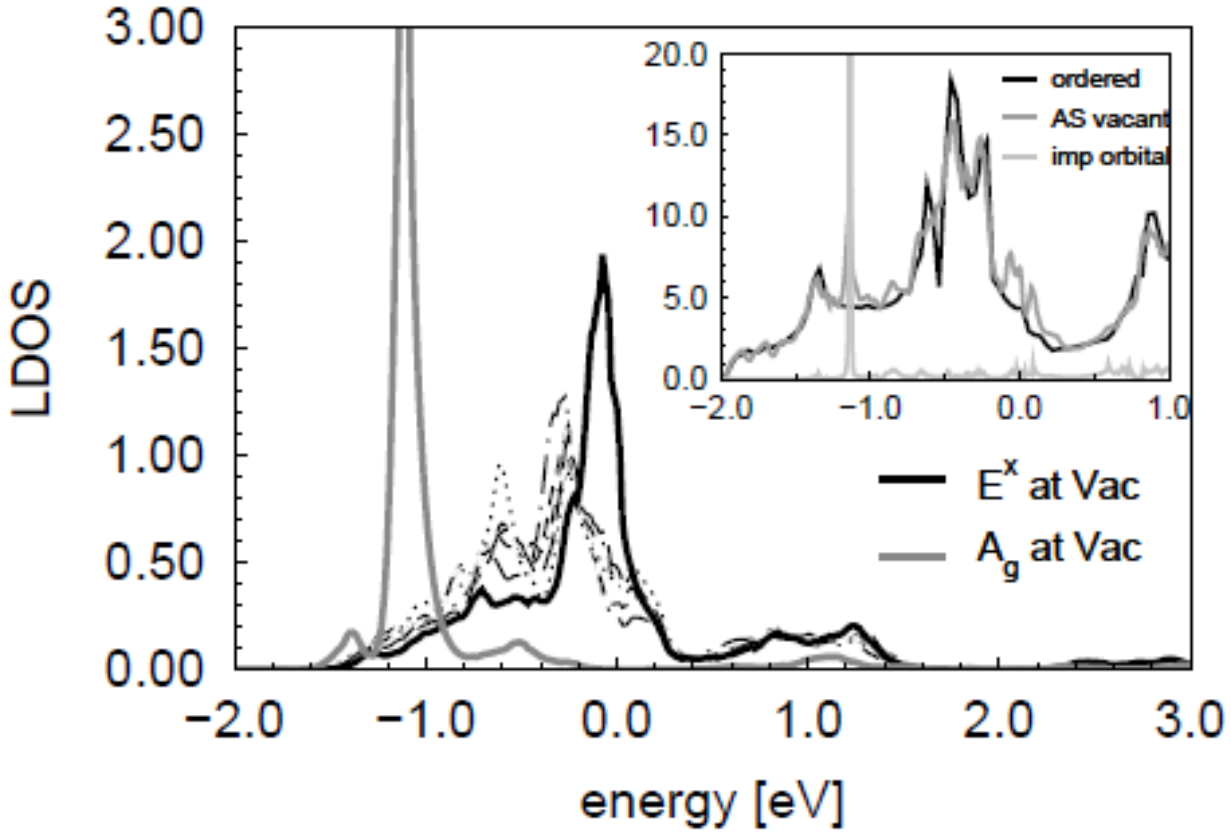

Figure 5: Molecular orbital projected LDOS. Black thick: E_x orbitals around the vacancy, Gray thick: A_g impurity state. Thin lines: E_x orbitals at other As sites. Inset: Black: total DOS ordered, medium grey: total DOS As-vacant, light grey: A_g impurity state empty orbital projection.

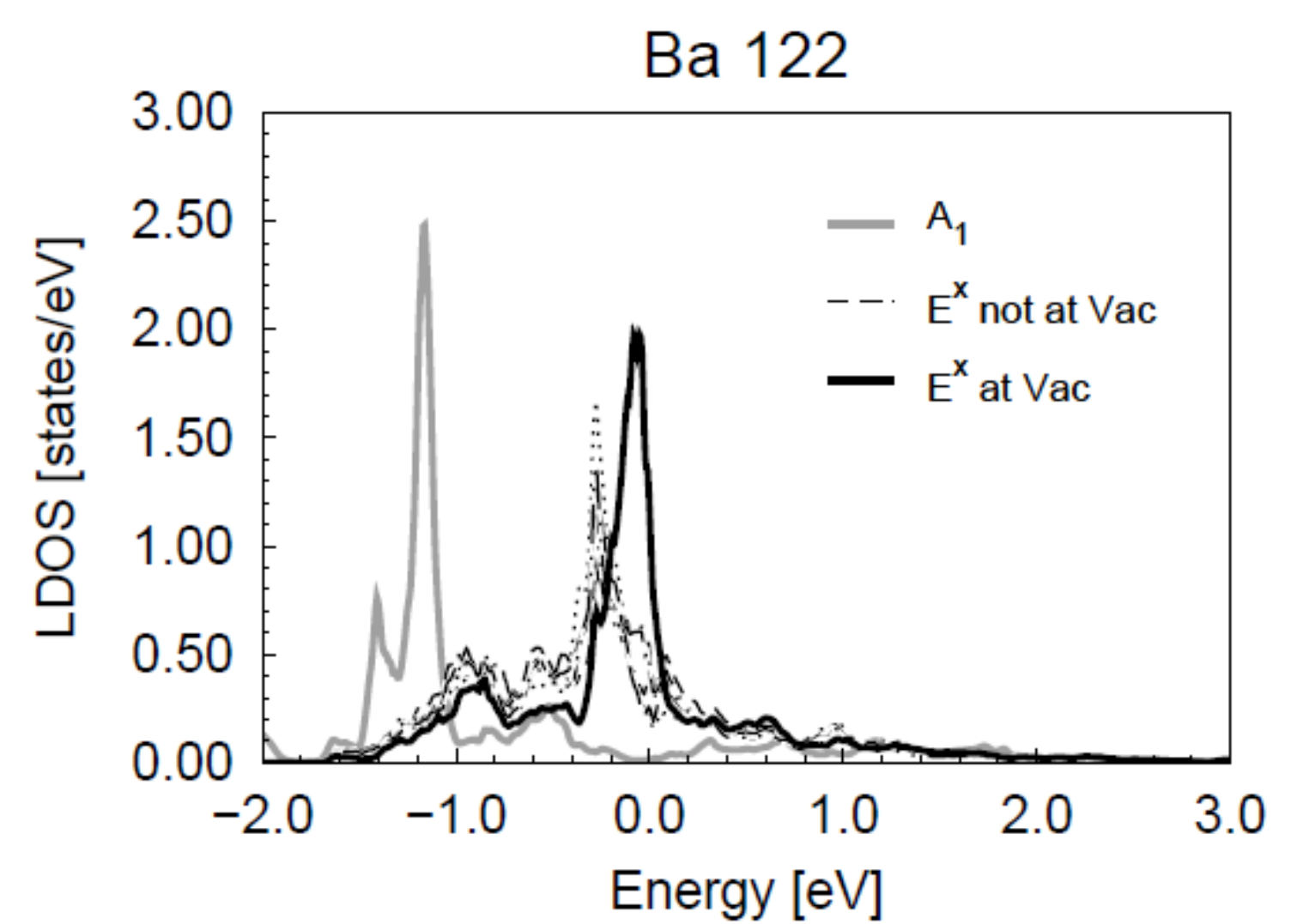
Ba 122
LDOS [states/eV]
3.00
2.50
2.00
1.50
1.00
0.50
0.00
−2.0
−1.0
0.0
1.0
2.0
3.0
Energy [eV]
A1
Ex not at Vac
Ex at Vac

Maximally projected Wannier functions: deep A_1 resonance

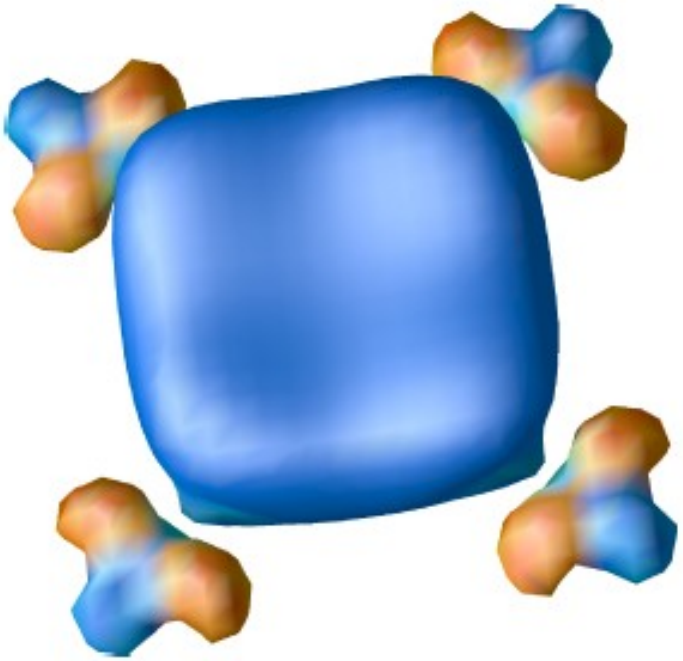

Figure 6: The A_g impurity state Wannier function. The As-vacancy sits at the center while the $3d$ lobs belong to the neighboring Fe atoms.

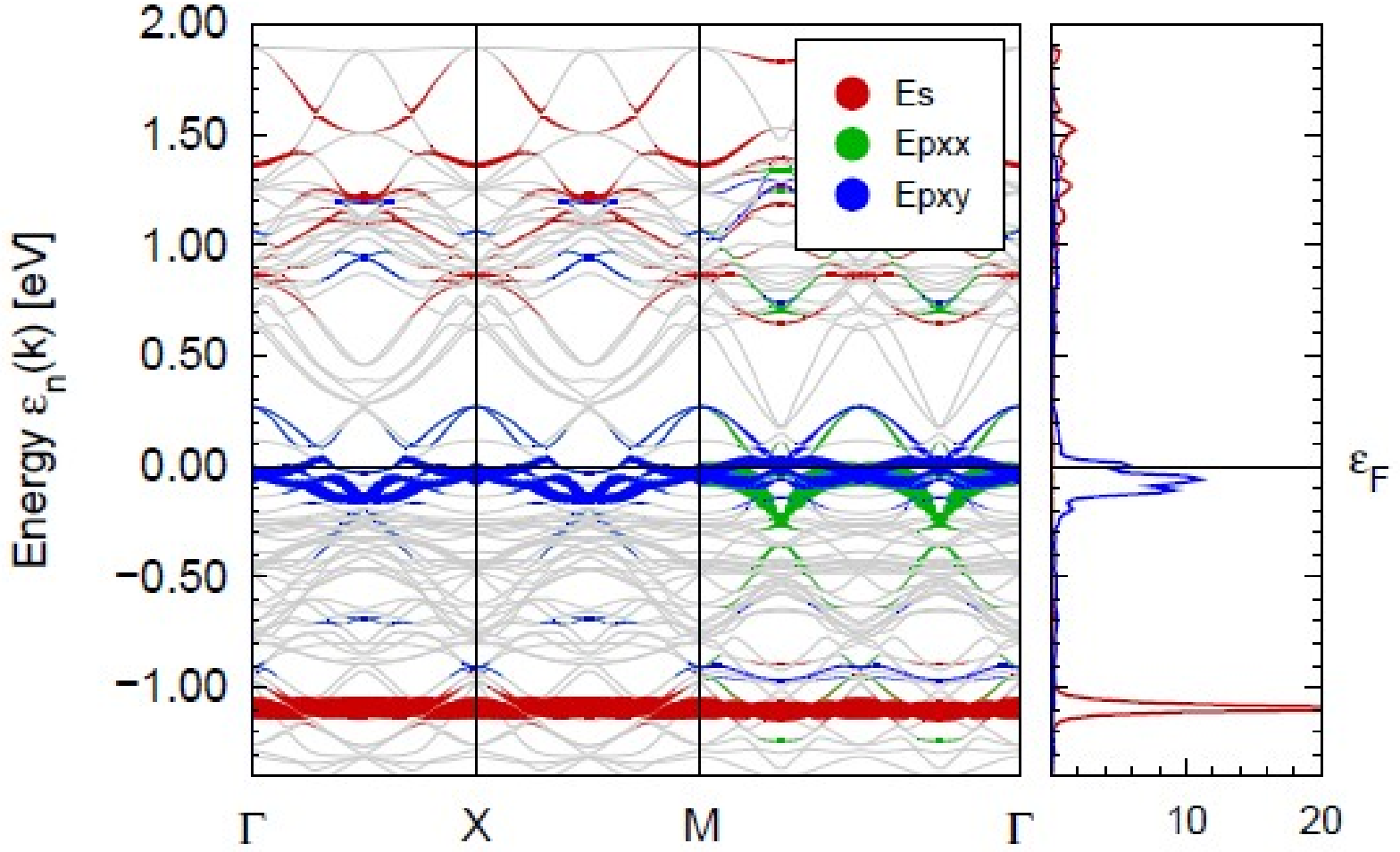

Figure 7: (color online) Wannier function bands and WF-LDOS of the A_g impurity state (light grey, red) and the E_x resonance (dark grey, blue).

To find the magnetic vacancy related state, we appeal to the
Wolff's model of localized moment in metal (***1961, in parallel to Anderson model***)

$$H = \sum_{\mathbf{k}b\sigma} \varepsilon_{\mathbf{k}b} d^{\dagger}_{\mathbf{k}b\sigma} d_{\mathbf{k}b\sigma} + W_{\beta} \sum_{i\beta\sigma} n_{i\beta\sigma} + \frac{I}{2} \sum_{i\beta\sigma} n_{i\beta\sigma} n_{i\beta\bar{\sigma}}$$

I is the "Hubbard" repulsion parameter for hybridized molecular orbitals |β> in the defect cluster. So, the eventual source of this interaction is the Hubbard repulsion I_0 on 4 Fe ions surrounding As vacancy. Spin-dependent scattering potential:

$$W_{\beta\sigma} = W_{\beta} + I\langle n_{\beta\bar{\sigma}} \rangle$$

Magnetic moment around defect may be formed provided $I > I_c$ estimated as

$$\frac{I_c}{E_B} \sim \frac{1}{2} + \frac{(\varepsilon_F - E_0)^2}{2\Gamma^2}$$

These paramagnetic "local" moments have itinerant origin. They are formed in the hole pocket on the background of FL with weak AFM spin fluctuation of SDW origin with characteristic wave vectors around $\boldsymbol{G}$.

Graphical solution of spin-dependent secular equation

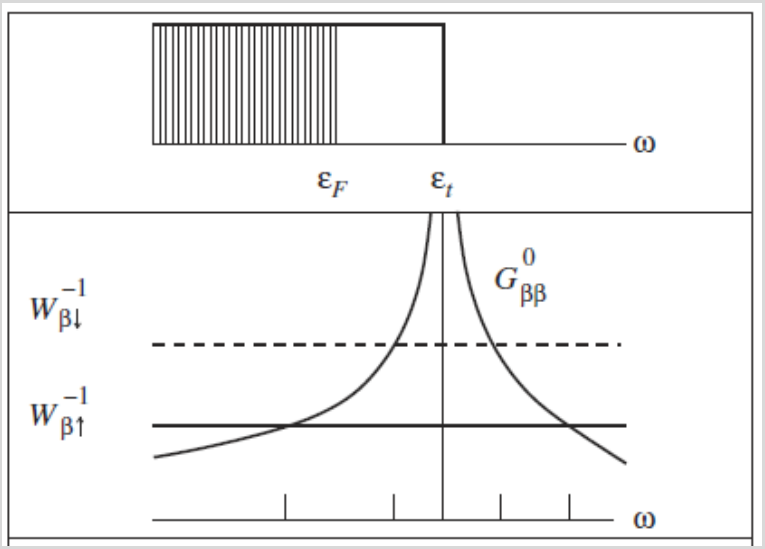

$$W_{\beta\sigma} = W_\beta + I\langle n_{\beta\bar{\sigma}}\rangle$$

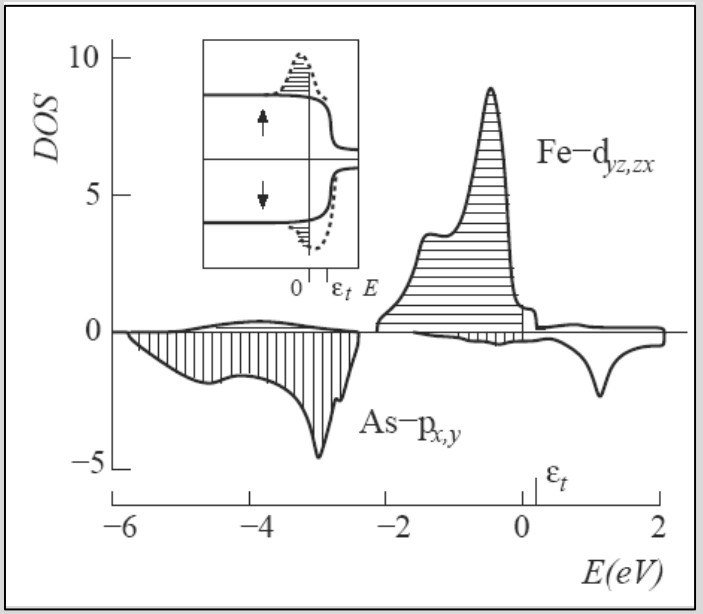

V_{As} induces magnetic moments at neighboring Fe ions

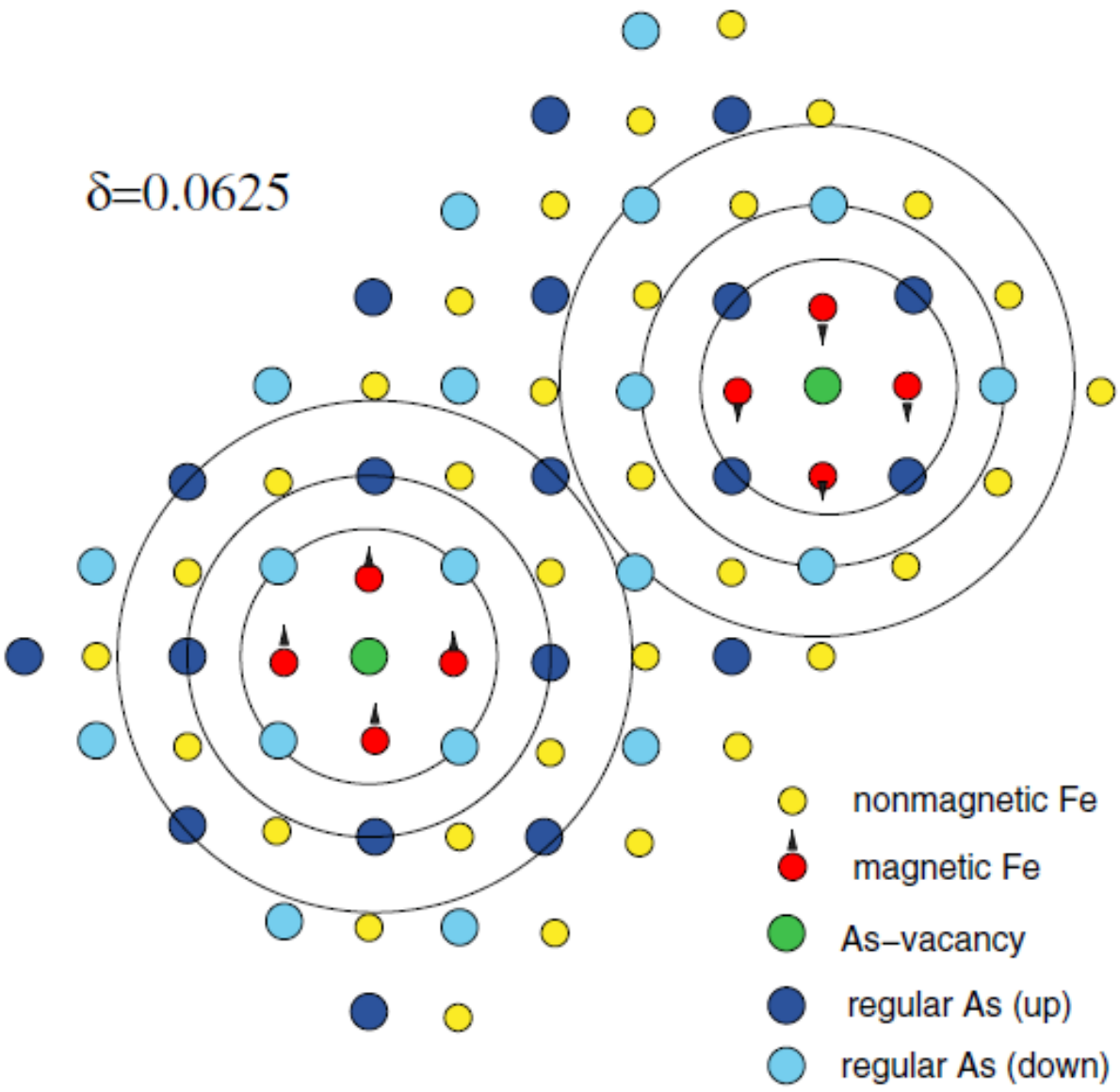

FIG. 2. (Color) Schematic structure of an FeAs block with two neighboring As-vacancies (AV) at a concentration of $\delta = 0.0625$,

Paramagnetic susceptibility
of a crystal with defects

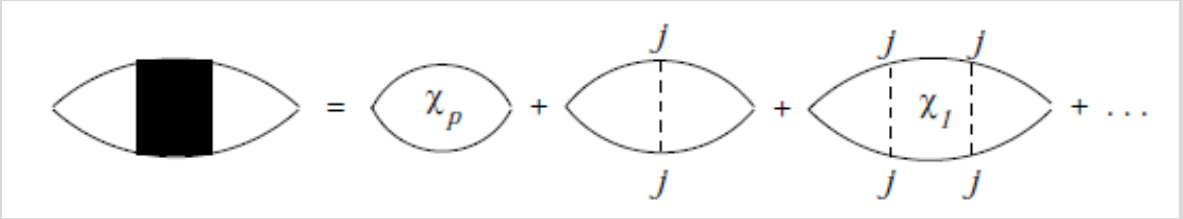

$$\chi = \chi_{\rm p}\left[1 + \frac{cI\chi_{\rm p}}{1 - I\chi_l}\right], \quad \chi_l = \langle S_j^+ S_j^- \rangle$$

Local enhancement is expected to be even stronger than the Stoner enhancement in pure crystals

This local enhancement explains experimental data of Grinenko et al

Fitting the experimental data gives the estimate of local Coulomb interaction in Fe_4 cluster around V_{As}

$I \sim 2.1 - 2.9$ eV, whereas $E_B \sim 3$-4 eV, so the Wolff criterion is satisfied.

We conclude that d-electrons in La-1111 system are on the verge of Mott-Hubbard transition but on the *itinerant* side of this transition. There are factors both detrimental for sc mode and favoring it. Apparently they nearly compensate each other.

In a sense As vacancy is a “smart” defect: it selectively perturbs the hole pockets (~*xz,yz*).
The theory predicts strong (resonance) magnetic scattering close to the unitarity limit of $\delta \sim \pi/2$ in the hole band and weak scattering ~ $\sin qa$ in the electron pocket, where ***q*** is the deviation from nesting conditions.

What about the influence of these “smart” defects on the superconductivity?

Two-mode theory of pairing instabilities

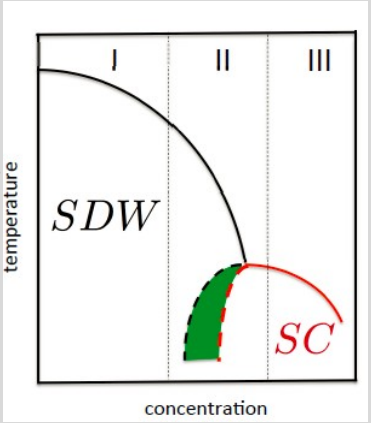

There are two competing soft modes at high temparatures close to T_c and/or T_s

$$\nu_0\Gamma_{\rm sc}(q,\omega,T) \to D_{\rm sc}(q,\omega) = \frac{\nu_0\Gamma^{(0)}_{sc}}{-\frac{i\omega}{\gamma_{sc}} + \tau_{\rm c} + a^2q^2}, \qquad (1)$$

$$\nu_0\Gamma_{\rm sdw}(\mathbf{Q}+\mathbf{q},\omega,T) \to D_{\rm sdw}(q,\omega) = \frac{\nu_0\Gamma^{(0)}_{sdw}}{-\frac{i\omega}{\gamma_{sdw}} + \tau_{\rm s} + b^2q^2}$$

with critical parameters

$$\tau_{\rm c} = \frac{T-T_c}{T_c}, \quad \tau_{\rm s} = \frac{T-T_{\rm s}}{T_{\rm s}}$$

$$\gamma_{sc/sdw} = 8T/\pi\ .$$

$$(aq)^2 \sim (bq)^2 \ll 1.$$

Starting from paramagnetic normal metal we do not appeal to any mean-field solution imposing an ordered state to the system but allow it to choose the type of ordering depending on the model parameters and doping degree.

As the pole Ω_i of the vertex part $\Gamma_{\rm sc}$ or $\Gamma_{\rm sdw}$ at $q \to 0$ tends to zero, the corresponding instability results in the phase transition.

These modes are coupled via the system of Bethe-Salpeter equation for vertex parts

Bethe-Salpeter equations for SDW, inter- and intraband Cooper pairing modes

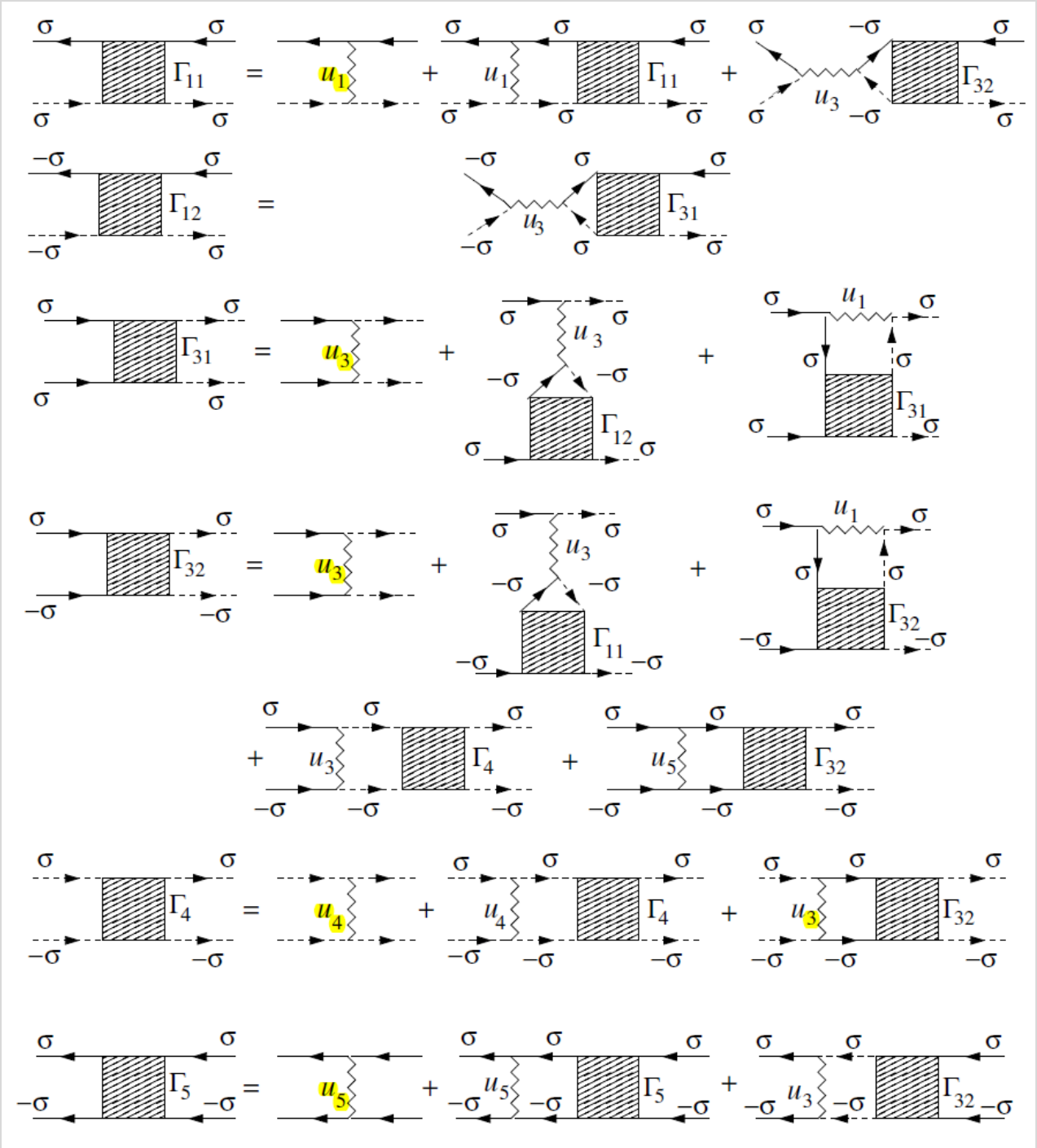

Bethe-Saltpeter equation for the interaction vertexes $u_{1\text{-}5}$
(*introduced by A. Chubukov et al)*

$$(1-\hat{\Lambda})\hat{\Gamma}=\hat{u}.$$

The matrix $(1-\hat{\Lambda})$ is the secular matrix and

$$\hat{u}=\begin{pmatrix} u_1 \\ u_3^{\sigma\bar{\sigma}} \\ u_3^{\sigma\sigma} \\ u_4 \\ u_5 \end{pmatrix}, \quad \hat{\Gamma}=\begin{pmatrix} \Gamma_{11} \\ \Gamma_{31} \\ \Gamma_{32} \\ \Gamma_4 \\ \Gamma_5 \end{pmatrix},$$

There are 5 coupled modes

$$\begin{aligned}
D_1^{-1} &= 1-u_1\Pi_1^{\sigma\sigma} \\
D_{31}^{-1} &= 1-u_1\Pi_1^{\sigma\sigma}-u_3^2\Pi_1^{\sigma\sigma}\Pi_1^{\bar{\sigma}\bar{\sigma}} \\
D_{32}^{-1} &= 1-u_1\Pi_1^{\sigma\sigma}-\left(u_4\Pi_4+u_5\Pi_5\right)/2 \\
D_4^{-1} &= 1-u_4\Pi_4 \\
D_5^{-1} &= 1-u_5\Pi_5
\end{aligned}$$

Solutions for the critical modes are found from the secular equation

$$\det(1-\hat{\Lambda}) = \begin{vmatrix} D_1^{-1}(p,\omega) & 0 & -u_3\Pi_1^{\bar{\sigma}\bar{\sigma}} & 0 & 0 \\ 0 & D_{31}^{-1}(p,\omega) & 0 & 0 & 0 \\ -u_3\Pi_1^{\bar{\sigma}\bar{\sigma}} & 0 & D_{32}^{-1}(p,\omega) & -u_3\Pi_4 & -u_3\Pi_5 \\ 0 & 0 & -u_3\Pi_5 & D_4^{-1}(p,\omega) & 0 \\ 0 & 0 & -u_3\Pi_4 & 0 & D_5^{-1}(p,\omega) \end{vmatrix} = 0$$

We assume $u_4\Pi_4 \ll 1$ and $u_5\Pi_5 \ll 1$

and simplify $u_4 = u_5,\ \Pi_4 = \Pi_5 = \Pi_s$

$$(1-\hat{\Lambda}') = \begin{pmatrix} D_1^{-1}(p,\omega) & -u_3\Pi_1^{\bar{\sigma}\bar{\sigma}} & 0 \\ -u_3\Pi_1^{\bar{\sigma}\bar{\sigma}} & D_{32}^{-1}(p,\omega) & -u_3\Pi_s \\ 0 & -u_3\Pi_s & D_s^{-1}(p,\omega) \end{pmatrix}$$

Interband SC and SDW modes are coupled with each other in presence of intraband SC pairing

Two susceptibilities responsible for instability of normal metallic phase are:

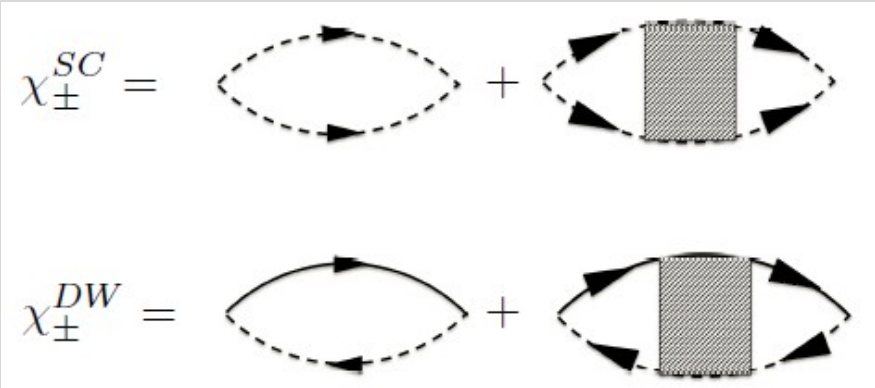

$$\chi^{SC}_{\pm,++}(\mathbf{k},T) = \frac{\Pi_4(\mathbf{k},T)}{1-(u_4 \pm u_3)\Pi_4(\mathbf{k},T)}.$$

$$\chi^{DW}_{\pm}(k,T) = \frac{\Pi_1(\mathbf{k},T)}{1-(u_1 \pm u_3)\Pi_1(\mathbf{k},T)}.$$

Mode crossing:

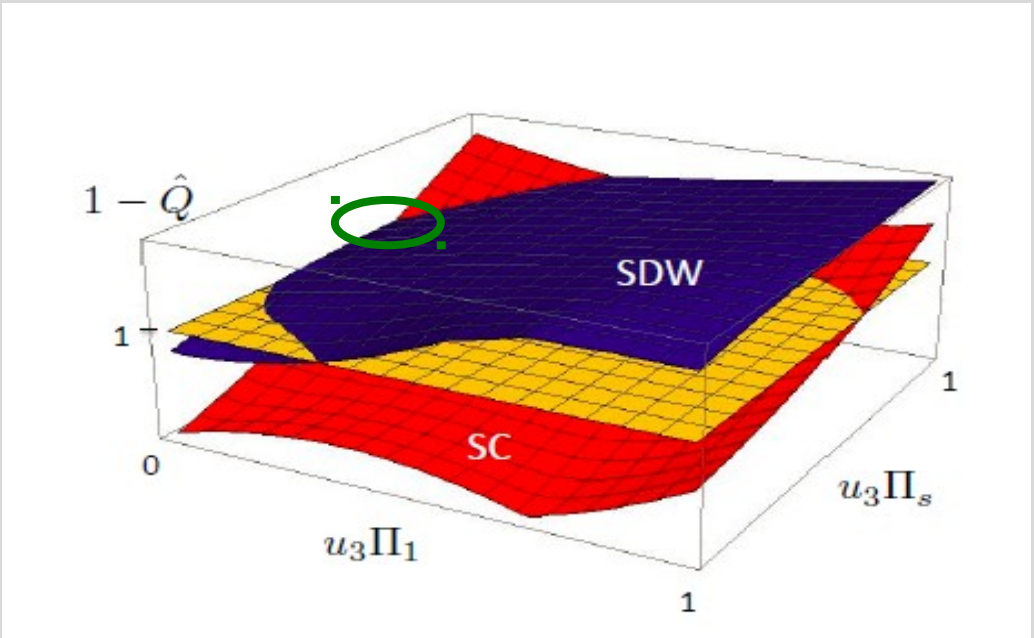

Mapping on the Ginzburg – Landau expansion

$$\delta\mathcal{F} = \alpha_\Delta |\Delta|^2 + \alpha_m \vec{m}^2 + A|\Delta|^4 + B\vec{m}^4 + 2C|\Delta|^2\vec{m}^2 + \ldots$$

$$\alpha_\Delta = 1/\chi_{\pm}^{(SC)}(\mathbf{k}=0,T) = \tfrac{1}{2}\ln(T/T_c)$$

$$\alpha_m = 1/\chi^{(SDW)}(\mathbf{k}=0,T)) = \tfrac{1}{2}\ln(T/T_s)$$

4th order terms are given by the the loops containing four Green's functions (***Vorontsov, Vavilov, Chubukov, 2010***)

Influence of “smart” magnetic defects on superconductivity

Vacancy related resonance scattering affects mode coupling via polarization loop Π_1

FIG. 3: Polarization loop Π_1 decorated by impurity scattering. Each filled circle corresponds to a vacancy defect represented by the T-matrix $\mathcal{T}^{\sigma}_{\mathbf{pp}'}(\varepsilon)$(18).

$$G_h(\varepsilon,\mathbf{pp}') = g_h(\varepsilon,p)\delta_{\mathbf{pp}'} + g_h(\varepsilon,p)\mathcal{T}(\mathbf{pp}',\varepsilon)g_h(\varepsilon,p') + \ldots,$$

$$\mathcal{T}^{\sigma}_{\mathbf{pp}',\varepsilon} = \frac{c_v F_\beta(\mathbf{p}) W_{\beta\sigma} F_\beta(\mathbf{p}')}{1 - W_{\beta,\sigma} G^0_{\beta\beta}(\varepsilon)} \quad \Rightarrow \quad \mathcal{T}^{\sigma}(\varepsilon) \approx \frac{c_v Z_\sigma}{\varepsilon - \varepsilon_{i\sigma} + i\gamma \mathrm{sgn}\varepsilon}$$

$$\delta\Pi_{1\sigma}(i\omega_m) = T\sum_n \sum_{\mathbf{p}} \delta G^{\sigma}_h(i\varepsilon_n,\mathbf{p}) g_e(i\varepsilon_n + i\omega_m, \mathbf{p}+\mathbf{q}) \sim \left((\epsilon_i - \epsilon_t)/\epsilon_t\right)^2$$

Only power law in comparison with logarighmically divergent main term,

Additional resonance scattering slightly shifts the crossing point and does not break pairs.

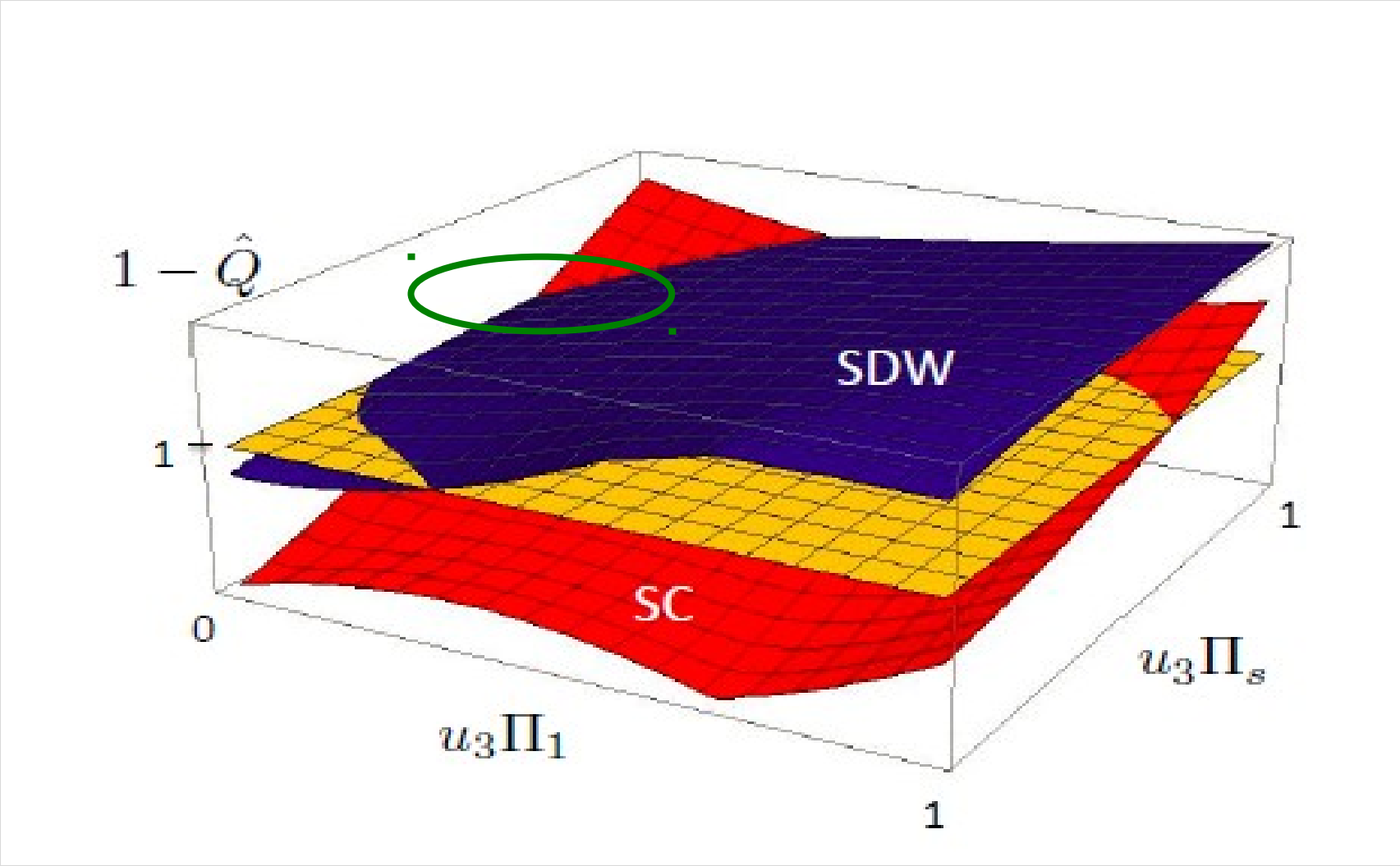
$1-\hat{Q}$
1
0
SDW
SC
$u_3\Pi_1$
1
$u_3\Pi_s$
1

* * *

Unlike V_{As}, Ru and Zn substitution impurities create dangling bonds within d-bands, so our analysis with some modification may be applied to those systems as well (*in progress*).

Zn^{2+} ($3d^{10}$) creates filled d-level ε_{di} well below iron related d-bands of a host crystal, whereas the 3d levels of Ru impurities are located well above those of Fe host.

In both cases dangling bonds around impurity form in 3d bands.

Both substitution core pontential and that of dangling bonds ~ $\delta\varepsilon = \varepsilon_{di} - \varepsilon_{dh}$.
This means that the defect potential is repulsive for Ru and attractive for Zn.

Toy 2D two-band model for impurities with dangling dd-bonds

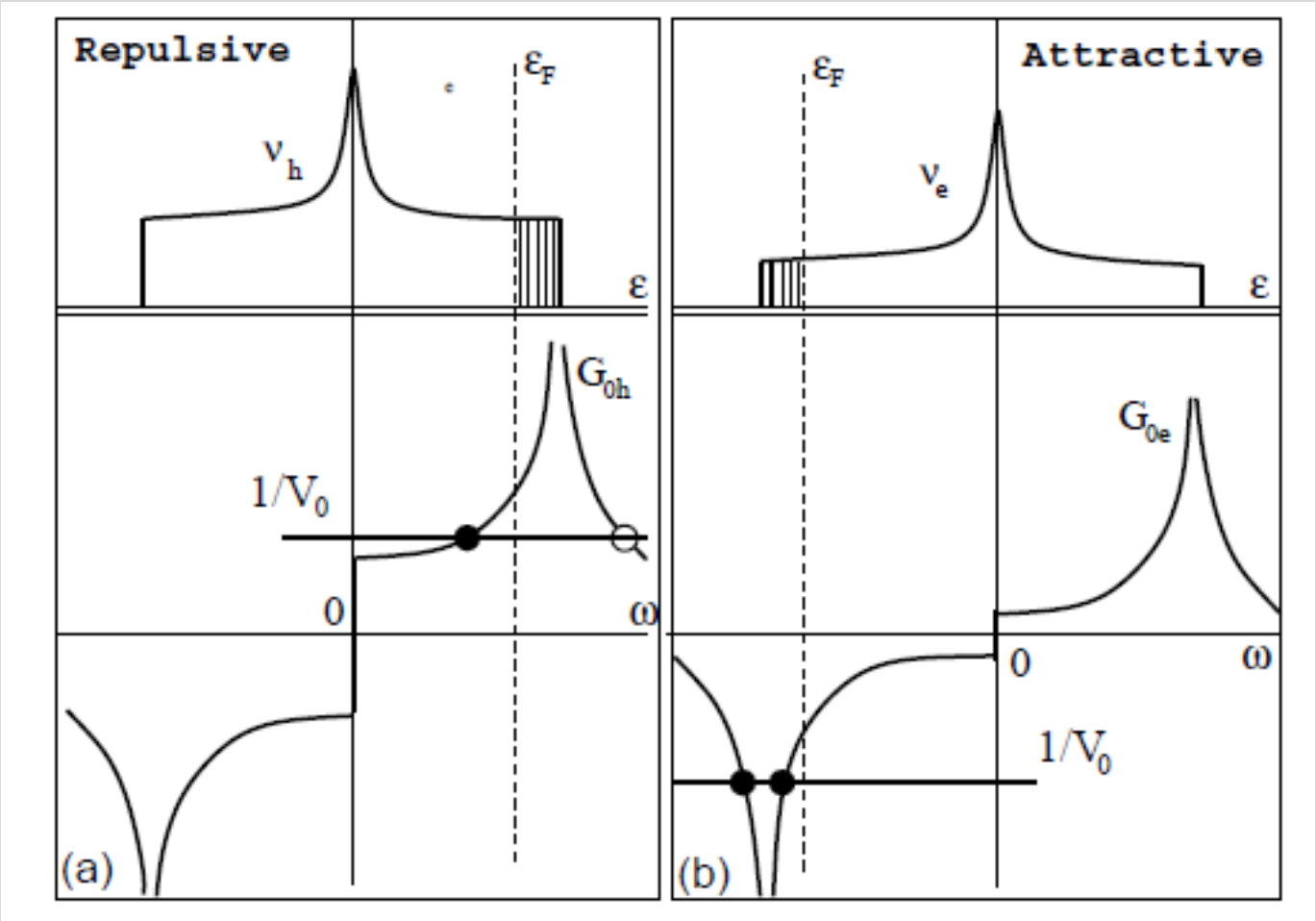

DOS

Solution of secular equation

$$1 - V_0 \hat{G}_0(\omega) = 0$$

Ru

Partially filled magnetic resonance

Zn

Filled resonance state (no magnetic moment)

To conclude:

- Weak effect of V_{As}-induced broken pd covalent bonds results in strong magnetic scattering due to quasi two-dimensionality of the bands and closeness of local paramagnetic response to Stoner instability.

- This "magnetic" defect manifests itself like unconventional *resonance* impurity in Cooper pairing via spin fluctuations.

- Other 'smart" bond breaking defects like Ru substituting for Fe may behave in a similar way.

•The contribution of resonance magnetic scattering may be incorporated in a two mode picture of competing SDW / SC fluctuations.

• The net contribution of "broken bonding" defects on T_c may be both positive and negative depending on specific situation in a given material

•Other modes (e.g. orbital mode of nematic fluctuations may be included in this scheme